Pharmacological Research 200 (2024) 107059

Contents lists available at ScienceDirect

Pharmacological Research

journal homepage: www.elsevier.com/locate/yphrs

Properties of FDA-approved small molecule protein kinase inhibitors: A 2024 update☆

Robert Roskoski Jr.

Blue Ridge Institute for Medical Research, 221 Haywood Knolls Drive, Hendersonville, NC 28791, United States

ARTICLE INFO

Keywords:
Alopecia areata
Breast cancer
Colorectal cancer
Chronic myelogenous leukemia
Mantle cell lymphoma
Myelofibrosis

ABSTRACT

Owing to the dysregulation of protein kinase activity in many diseases including cancer, this enzyme family has become one of the most important drug targets in the 21st century. There are 80 FDA-approved therapeutic agents that target about two dozen different protein kinases and seven of these drugs were approved in 2023. Of the approved drugs, thirteen target protein-serine/threonine protein kinases, four are directed against dual specificity protein kinases (MEK1/2), twenty block nonreceptor protein-tyrosine kinases, and 43 inhibit receptor protein-tyrosine kinases. The data indicate that 69 of these drugs are prescribed for the treatment of neoplasms. Six drugs (abrocitinib, baricitinib, deucravacitinib, ritlecitinib, tofacitinib, upadacitinib) are used for the treatment of inflammatory diseases (atopic dermatitis, rheumatoid arthritis, psoriasis, alopecia areata, and ulcerative colitis). Of the 80 approved drugs, nearly two dozen are used in the treatment of multiple diseases. The following seven drugs received FDA approval in 2023: capivasertib (HER2-positive breast cancer), fruquintinib (metastatic colorectal cancer), momelotinib (myelofibrosis), pirtobrutinib (mantle cell lymphoma, chronic lymphocytic leukemia, small lymphocytic lymphoma), quizartinib (*Flt3*-mutant acute myelogenous leukemia), repotrectinib (ROS1-positive lung cancer), and ritlecitinib (alopecia areata). All of the FDA-approved drugs are orally effective with the exception of netarsudil, temsirolimus, and trilaciclib. This review summarizes the physicochemical properties of all 80 FDA-approved small molecule protein kinase inhibitors including the molecular weight, number of hydrogen bond donors/acceptors, polar surface area, potency, solubility, lipophilic efficiency, and ligand efficiency.

1. The importance of therapeutic protein kinase inhibitors

Because of genetic alterations including translocations and mutations as well as overexpression, the dysregulation of protein kinase activity plays a significant role in the pathogenesis of autoimmune, inflammatory, cardiovascular, and nervous diseases as well as a number of malignancies. Accordingly, protein kinases are among the most important drug targets in the 21st century [1,2]. Perhaps a quarter to a third of drug development efforts in the United States and worldwide target these enzymes. The clinical effectiveness of imatinib in the treatment of Philadelphia chromosome-positive CML (chronic myelogenous leukemia) in 2001 prompted the search for orally effective therapeutic protein kinase blockers [3–5]. This extraordinary success resulted from the imatinib inhibition of the active chimeric BCR-Abl protein-tyrosine kinase, the causative biochemical defect that produces these leukemias.

Abbreviations: ACVR1, activin receptor type 1; AML, acute myelogenous leukemia; AS, activation segment; BMP, bone morphogenetic protein; BP, back pocket; C-spine, catalytic spine; CS1, catalytic spine residue 1; CML, chronic myelogenous leukemia; CL, catalytic loop; CRC, colorectal cancer; EGFR, epidermal growth factor receptor; ER, estrogen receptor; FDA, the Food and Drug Administration of the United States; FP, front pocket; FGFR, fibroblast growth factor receptor; GK, gatekeeper; GRL, glycine-rich loop; HER2, human epidermal growth factor receptor-2; JAK, Janus kinase; KLIFS, kinase-ligand interaction fingerprint and structure; LE, ligand efficiency; LipE, lipophilic efficiency; NF, nuclear factor; NSCLC, non-small cell lung cancer; PDGFR, platelet-derived growth factor receptor; PI3K, phosphatidylinositol 3-kinase; $PIP_{2,}$, phosphatidylinositol 4,5-bisphosphate; PIP_3, phosphatidylinositol 3,4,5-trisphosphate; PKA, protein kinase A; PLC, phospholipase C; PSA, polar surface area; Ro5, Lipinski's rule of five; R-spine, regulatory spine; RS1, regulatory spine residue 1; Sh2, shell residue 2; SMAD, suppressor of mothers against decapentaplegic; STAT, signal transducer and activator of transcription; VEGFR, vascular endothelial growth factor receptor.

☆ Chemical compounds studied in this article: Capivasertib (PubChem CID: 25227436); Fruquintinib (PubChem CID: 44480399); Momelotinib (PubChem CID: 25062766); Pirtobrutinib (PubChem CID: 129269915); Quizartinib (PubChem CID: 24889392); Imatinib (PubChem CID: 5291); Repotrectinib (PubChem CID: 135565923); Ritlecitinib (PubChem CID: 118115473); Sorafenib (PubChem CID: 216239); Sunitinib (PubChem CID: 5329102)

E-mail address: rrj@brimr.org.

https://doi.org/10.1016/j.phrs.2024.107059
Received 3 January 2024; Accepted 4 January 2024
Available online 11 January 2024
1043-6618/© 2024 The Author(s). Published by Elsevier Ltd. This is an open access article under the CC BY-NC-ND license (http://creativecommons.org/licenses/by-nc-nd/4.0/).

The inventory of several thousand protein kinase X-ray crystal structures in the public domain accelerated structure-based drug development. Moreover, additional proprietary structures solved by commercial ventures are in widespread use in the drug development process. Approximately 180 orally effective protein kinase inhibitors are in clinical trials worldwide [6]. A comprehensive listing of these agents, which is regularly updated, can be obtained at www.icoa.fr/pkidb/. There are 80 FDA-approved drugs that target about two dozen different protein kinases (see Table 1 and supplementary material). These protein kinases, nonetheless, represent a small fraction of the 518-member protein kinase enzyme superfamily. Additional medicinals directed against these and other protein kinases are in clinical trials in the United States and across the globe [4–7].

Manning et al. reported that the human protein kinase superfamily contains 478 typical and 40 atypical enzymes [8] including phosphatidylinositol 3-kinase (PI3K) [5,9]. Protein kinases mediate the following reaction;.

$$MgATP^{1-} + \text{protein–O:H} \rightarrow \text{protein–O:}PO_3^{2-} + MgADP + H^+$$

Based upon the nature of the protein–OH groups, these catalysts are divided into protein-tyrosine kinases (90 members), protein-tyrosine kinase–like enzymes (43), and protein-serine/threonine kinases (385). The protein-tyrosine kinase family consists of both intracellular nonreceptor (32) and transmembrane receptor (58) proteins. Moreover, the protein kinase family includes a small group of intracellular enzymes such as MEK1/2 that catalyze the phosphorylation of both tyrosine and then threonine residues within the activation segment of their target protein kinases; because of this unique action, MEK1/2 and related enzymes are called dual specificity protein kinases. Another indication of the importance of the protein kinase family is the estimate that about one in every 40 human genes (518 protein kinase genes out of an estimated 20,000 human protein-encoding genes) encodes a protein kinase. Protein kinases consequently constitute about 2.5% of the human genome. Additional evidence for the importance of protein kinases as drug targets is the finding of Manning et al. that suggests that 244 protein kinases map to cancer amplicons and other disease loci [8]. Accordingly, as additional research on the pathogenesis of various diseases is performed, it is quite likely that there will be a notable increase in the number of protein kinase therapeutic targets.

Table 1
Principal FDA-approved protein kinase inhibitor drug targets.

Kinase family	Class of Kinase	US FDA approved
EGFR/ErbB	RY	10
JAK	NRY	9
VEGFR	RY	9
BCR-Abl	NRY	6
ALK	RY	5
FGFR	RY	5
CDK4/6	S/T	4
MEK1/2	Y/T	4
BTK	NRY	4
BRAF	S/T	3
FKBP	S/T	3
Flt3	RY	3
MET	RY	3
RET	RY	2
ROCK	S/T	2
TRKA	RY	2
CSF1	RY	1
Kit	RY	1
PDGFR	RY	1
ROS1	RY	1
SYK	RY	1
TYK2	NRY	1
Total		80

NYR, nonreceptor protein-tyrosine kinase; RY, receptor protein-tyrosine kinase; S/T, protein-serine/threonine kinase; Y/T, Dual specificity protein kinase – tyrosine phosphorylation followed by threonine phosphorylation of target kinase activation segments

The FDA has approved 80 small molecule therapeutic protein kinase inhibitors as of 1 January 2024 (Table 2) [10–13], nearly all of which are orally effective with the exceptions of netarsudil (an eye drop) and temsirolimus and trilaciclib (which are given intravenously). Ruxolitinib is an orally effective JAK1/2 therapeutic protein kinase antagonist that was approved for the treatment of myelofibrosis and polycythemia vera in 2011. This compound is topically active as a cream and was approved in 2021 for the treatment of atopic dermatitis. Of the 80 approved drugs, forty-three target receptor protein-tyrosine kinases, twenty inhibit nonreceptor protein-tyrosine kinases, thirteen antagonize protein-serine/threonine protein kinases, and four target dual specificity protein kinases (MEK1/2) (Table 1). The data indicate that 69 of these medicinals are approved for the management of solid and nonsolid neoplasms. Two drugs (ibrutinib, belumosudil) are approved for the treatment of graft vs. host disease and three drugs (upadacitinib, tofacitinib, baricitinib) are prescribed for the treatment of rheumatoid arthritis. More than two dozen of the approved drugs are multikinase antagonists. Because the specificity of many of the protein kinase inhibitors has not been rigorously assessed, it is probable that many more of the approved drugs are multikinase inhibitors. The concurrent inhibition of several protein kinases has potential advantages and disadvantages. For example, the therapeutic effectiveness of multikinase blockers may be related to the inhibition of two or more targets. Sunitinib and cabozantinib, for example, have potent off-target activity against the Axl receptor protein-tyrosine kinase and this property may add to their clinical efficacy [14]. In contrast, the blockade of off-target kinases may elicit unwanted side effects. Consequently, we have the dilemma of whether a magic shotgun should be preferred to Paul Ehrlich's magic bullet [15].

Eleven of the FDA-approved protein kinase antagonists are used for the treatment of nonneoplastic diseases. For example, (i) netarsudil is employed for the treatment of glaucoma, (ii) sirolimus and belumosudil are used for the management of graft vs. host disease, (iii) nintedanib is prescribed for the treatment of idiopathic pulmonary fibrosis, (iv) fostamatinib is used for the treatment of chronic immune thrombocytopenia, (v) baricitinib and upadacitinib are prescribed for the management of rheumatoid arthritis, (vi) ruxolitinib and abrocitinib are used for the treatment of atopic dermatitis, (vii) tofacitinib is employed for the management of psoriatic arthritis, rheumatoid arthritis, and ulcerative colitis, and (viii) upadacitinib is employed for the treatment of psoriatic arthritis, rheumatoid arthritis, and atopic dermatitis [10–13]. Furthermore, ibrutinib and sirolimus are approved therapeutics for both neoplastic and nonneoplastic diseases.

Eight of the FDA-approved kinase inhibitors form covalent bonds with their target enzymes and they are accordingly classified as TCIs (targeted covalent inhibitors) [16]. These agents include acalabrutinib (blocking BTK in mantle cell lymphoma), dacomitinib (targeting mutant *EGFR* in NSCLC), osimertinib (antagonizing *EGFR T970M* mutants in NSCLC), afatinib (blocking EGFR in NSCLC), neratinib (inhibiting ErbB2 in HER2-positive breast cancer), zanubrutinib (blocking BTK in mantle cell lymphoma), ritlecitinib (targeting JAK3 in alopecia areata), and ibrutinib (inhibiting BTK in chronic lymphocytic leukemia, mantle cell lymphoma, marginal zone lymphoma, chronic graft vs. host disease, and Waldenström macroglobulinemia). The closely related EGFR and ErbB4 of the ErbB1/2/3/4 epidermal growth factor receptor family are the most common protein kinases bearing mutations in all cancers [3]. For a summary of the characteristics of small molecule protein kinase blockers that were approved by the FDA prior to 2023, see Refs. [10–13,17].

Of the 80 FDA-approved protein kinase inhibitors, twenty-seven are prescribed for the treatment of more than one disease. For example, imatinib is approved for the management of eight distinct maladies (Table 2). This medicine inhibits the nonreceptor protein-tyrosine kinase Abl (and the BCR-Abl chimera – responsible for the pathogenesis of chronic myelogenous leukemia), Abl2, PDGFRα/β, Kit (the stem cell factor receptor), and epithelial discoidin domain-containing receptor-1

Table 2
FDA-approved small molecule protein kinase inhibitors, their protein kinase targets, and therapeutic indications[a].

Drug	Code	Company	Trade name	Year approved	Primary targets[b]	Therapeutic indications[c]
Abemaciclib	LY2835219	Lilly	Verzenio	2017	CDK4/6	HER2-positive breast cancer, both monotherapy and combination therapy
Abrocitinib	PF-04965842	Pfizer	Cibinqo	2022	JAK1	Atopic dermatitis
Acalabrutinib	ACP-196	Acerta Pharma	Calquence	2017	BTK	Mantle cell lymphoma, chronic lymphocytic leukemia, small lymphocytic lymphoma
Afatinib	BIBW 2992	Boehringer Ingelheim	Tovok	2013	ErbB1/2/4	NSCLC (non-small cell lung cancer) and squamous NSCLC
Alectinib	CH5424802	Roche	Alecensa	2015	ALK, RET	Third-line Ph^+ chronic myelogenous leukemia (CML) and CML with *T315I* mutations
Asciminib	ABL001	Novartis	Scemblix	2021	BCR-Abl	Ph^+ CML
Avapritinib	BLU285	Blueprint Medicines	Ayvakit	2020	PDGFRα	Gastrointestinal stromal tumors with a *PDGFRα* exon 18 mutation
Axitinib	AG-013736	Pfizer	Inlyta	2012	VEGFR1/2/3	Advanced renal cell carcinoma
Baricitinib	LY 3009104	Lilly	Olumiant	2018	JAK1/2	Rheumatoid arthritis
Belumosudil	KD025	Kadmon Pharma	Rezurock	2021	ROCK2	Graft vs. host disease
Binimetinib	MEK162	Array BioPharma	Mektovi	2018	MEK1/2	Melanoma with *BRAF V600E* or *V600K* mutations with encorafenib
Bosutinib	SKI-606	Pfizer	Bosulif	2012	BCR-Abl	Ph^+ chronic myelogenous leukemia
Brigatinib	AP 26113	Ariad Pharm	Alunbrig	2017	ALK	ALK-positive NSCLC
Cabozantinib	BMS-907351	Exelixis	Cometriq & Cabometyx	2012	RET, VEGFR2	Advanced medullary thyroid cancer, renal cell and hepatocellular carcinomas
Capivasertib	AZD5363	AstraZeneca	Truqap	2023	HER2	Hormone receptor (HR)-positive, human epidermal growth factor receptor 2 (HER2)-negative breast cancer
Capmatinib	INC-280	Novartis	Tabrecta	2020	MET (HGFR)	NSCLC with *MET* exon 14 skipping mutations
Ceritinib	LDK378	Novartis	Zykadia	2014	ALK	ALK-positive NSCLC resistant to crizotinib
Cobimetinib	GDC-0973	Genentech	Cotellic	2015	MEK1/2	*BRAF V600E or V600K* mutation positive melanomas in combination with vemurafenib
Crizotinib	PF 2341066	Pfizer	Xalkori	2011	ALK, ROS1	ALK- or ROS1-postive NSCLC
Dabrafenib	GSK2118436	GSK	Tafinlar	2013	BRAF	*BRAF* mutation positive melanoma, NSCLC with *BRAF V600E* mutations, anaplastic thyroid cancer with *BRAF V600E* mutations
Dacomitinib	PF-00299804	Pfizer	Visimpro	2018	EGFR	*EGFR*-mutant NSCLC
Dasatinib	BMS-354825	Bristol Myers Squibb	Sprycel	2006	BCR-Abl	Ph^+ chronic myelogenous leukemia or acute lymphoblastic leukemia
Deucravacitinib	BMS-986165	Bristol Myers Squibb	Sotyktu	2022	TYK2	Psoriasis
Encorafenib	LGX818	Array BioPharma	Braftovi	2018	BRAF	*BRAF V600E* or *V600K* mutation positive melanoma with binimetinib; *BRAF V600E* mutation positive colorectal cancer with cetuximab
Entrectinib	RXDX-101	Genentech	Rozlytrek	2019	TRKA/B/C, ROS1	Solid tumors with NTRK fusion proteins, ROS1-positive NSCLC
Erdafitinib	JNJ-42756493	Jansen Pharm	Balversa	2019	FGFR1/2/3/4	Urothelial bladder cancer
Erlotinib	OSI-774	Genentech	Tarceva	2004	EGFR	NSCLC, pancreatic cancer
Everolimus	RAD001	Novartis	Afinitor	2009	FKBP12/mTOR	HER2-negative breast cancer, pancreatic neuroendocrine tumors, RCC, angiomyolipoma, subependymal giant cell astrocytoma
Fedratinib	TG101348	Celgene	Inrebic	2019	JAK2	Myelofibrosis
Fostamatinib	R788	Rigel Pharma.	Tavalisse	2018	SYK	Chronic immune thrombocytopenia
Fruquintinib	HMPL013	Takeda	Fruzaqla	2023	VEGFR2	Metastatic colorectal cancer
Futibatinib	TAS_120	Tiaho Pharma	Lytgobi	2022	FGFR2	Bile duct cancers (cholangiocarcinomas) with FGFR2 fusion proteins or other rearrangements
Gefitinib	ZD1839	AstraZeneca	Iressa	2003	EGFR	NSCLC with exon 19 deletions or exon 21 substitutions
Gilteritinib	ASP2215	Astellas Pharma	Xospata	2018	Flt3	*FLT3*-mutation positive acute myeloid leukemia
Ibrutinib	PCI-32765	Johnson & Johnson	Imbruvica	2013	BTK	Chronic lymphocytic leukemia, mantle cell lymphoma, marginal zone lymphoma, graft vs. host disease, Waldenström macroglobulinemia
Imatinib	STI571	Novartis	Gleevec	2001	BCR-Abl	Ph^+ chronic myelogenous leukemia or acute lymphoblastic leukemia, aggressive systemic mastocytosis, chronic eosinophilic leukemia, dermatofibrosarcoma protuberans, hypereosinophilic syndrome, gastrointestinal stromal tumors, myelodysplastic/myeloproliferative disease
Infigratinib	BGJ 398	QED Therapeutics	Truseltiq	2021	FGFR2	Cholangiocarcinomas with FGFR2 fusions or other rearrangement
Lapatinib	GW572016	GSK	Tykerb	2007	EGFR, ErbB2/HER2	HER2-positive breast cancer
Larotrectinib	LOXO-101	Bayer	Vitrakvi	2018	TRKA/B/C	Solid tumors with NTRK fusion proteins
Lenvatinib	AK175809	Easai Co.	Lenvima	2015	VEGFR, RET	Differentiated thyroid cancer, hepatocellular carcinoma, renal cell carcinoma, endometrial carcinoma
Lorlatinib	PF-06463922	Pfizer	Lorbrena	2018	ALK	ALK-positive NSCLC
Midostaurin	CPG 41251	Novartis	Rydapt	2017	Flt3	*FLT3* mutation positive AML, mastocytosis, mast cell leukemia
Mobocertinib	TAK-788	Takeda Pharm.	Exkivity	2021	EGFR	NSCLC with *EGFR*-positive exon 20 insertions
Momelotinib	CYT 387	GSK	Ojjaara	2023	JAK2	Myelofibrosis patients with anemia

(*continued on next page*)

Table 2 (*continued*)

Drug	Code	Company	Trade name	Year approved	Primary targets[b]	Therapeutic indications[c]
Neratinib	HKI-272	Puma Biotech	Nerlynx	2017	ErbB2/HER2	HER2-positive breast cancer
Netarsudil	AR11324	Aerie Pharma	Rhopressa	2018	ROCK1/2	Glaucoma
Nilotinib	AMN107	Novartis	Tasigna	2007	BCR-Abl	Ph^+ chronic myelogenous leukemia
Nintedanib	BIBF-1120	Boehringer Ingelheim	Vargatef	2014	FGFR1/2/3	Idiopathic pulmonary fibrosis
Osimertinib	AZD-9292	AstraZeneca	Tagrisso	2015	EGFR	NSCLC with exon 19 or exon 21 substitutions (L858R) or T790M mutations
Pacritinib	SB1518	CTI BioPharma	Vonjo	2022	JAK2	Myelofibrosis
Palbociclib	PD-0332991	Parke-Davis	Ibrance	2015	CDK4/6	Breast cancer (HER2-positive or negative) combination therapy
Pazopanib	GW786034	GSK	Votrient	2009	VEGFR1/2/3	Renal cell carcinoma, soft tissue sarcomas
Pemigatinib	INCB054828	Incyte Corp.	Pemazyre	2020	FGFR2	Advanced cholangiocarcinoma with FGFR2 fusions or rearrangements
Pexidartinib	PLX3397	Plexxikon Inc	Turalio	2019	CSF1R	Tenosynovial giant cell tumors
Pirtobrutinib	LOXO-305	Lilly	Jaypirca	2023	BTK	Mantle cell lymphoma, chronic lymphocytic leukemia, small lymphocytic lymphoma
Ponatinib	AP 24534	Ariad Pharm	Iclusig	2012	BCR-Abl	Ph^+ chronic myelogenous leukemia, acute lymphoblastic leukemia
Pralsetinib	Blu-667	Blueprint Medicines	Gavreto	2020	RET	RET-fusion protein NSCLC, RET mutant medullary thyroid cancer, RET fusion thyroid cancer
Quizatinib	ASP-2869	Daiichi Sankyo	Vanflyta	2023	Flt3	*FLT3* internal tandem duplication positive acute myelogenous leukemia in combination with cytarabine and daunorubicin
Regorafenib	BAY 73-4506	Bayer	Stivarga	2012	VEGFR1/2/3	Colorectal cancer, hepatocellular carcinoma, gastrointestinal stromal tumors
Repotrectinib	TX-0005	Bayer	Augtyro	2023	ROS1	ROS1-positive NSCLC
Ribociclib	LEE011	Novartis	Kisqali	2017	CDK4/6	Breast cancer (HER2-positive or negative) combination therapy
Ripretinib	DCC-2618	Decipera Pharma.	Qinlock	2020	Kit, PDGFRα	Fourth-line treatment for gastrointestinal stromal tumors
Ritlecitinib	PF06651600	Pfizer	Litfulo	2023	JAK3	Alopecia areata
Ruxolitinib	INCB-018424	Incyte Corp.	Jakafi	2011	JAK1/2/3, TYK	Myelofibrosis, polycythemia vera, graft vs. host disease, atopic dermatitis (applied topically)
Selpercatinib	CEGM9YBNG	Lilly	Retevmo	2020	RET	RET fusion NSCLC, RET fusion solid tumors, RET fusion thyroid cancers and *RET* mutant medullary thyroid cancer
Selumetinib	AZD6224	AstraZeneca	Koselugo	2020	MEK1/2	Neurofibromatosis type I
Sirolimus	AY 22989	Wyeth, LLC	Rapamycin	1999	FKBP12/mTOR	Kidney transplant, lymphangioleiomyomatosis
Sorafenib	BAY 43-9006	Bayer	Nexavar	2005	VEGFR1/2/3	Hepatocellular carcinoma, renal cell carcinoma, differentiated thyroid cancer
Sunitinib	SU11248	Pfizer	Sutent	2006	VEGFR2	Gastrointestinal stromal tumors, renal cell carcinoma, pancreatic neuroendocrine tumors
Temsirolimus	CCI-779	Wyeth, LLC	Torisel	2007	FKBP12/mTOR	Advance renal cell carcinoma
Tepotinib	EMD 1214063	EMD Serono Inc.	Tepmetko	2021	MET (HGFR)	*MET*-mutant NSCLC
Tivozanib	AV951	AVEO Pharma	Fotvida	2021	VEGFR2	Third-line treatment of renal cell carcinoma
Tofacitinib	CP-690550	Pfizer	Tasocitinib	2012	JAK3	Rheumatoid arthritis, psoriatic arthritis, ulcerative colitis
Trametinib	GSK1120212	GSK	Mekinist	2013	MEK1/2	Melanoma with *BRAF V600E* or *V600K* mutations with dabrafenib; NSCLC with *BRAF V600E* mutations with dabrafenib
Trilaciclib	G1T28	G1 Therapeutics	Cosela	2021	CDK4/6	Chemotherapy-induced myelosuppression when administered prior to a platinum/etoposide-containing regimen or topotecan-containing regimen for extensive-stage small cell lung cancer
Tucatinib	ONT-380	Seattle Genetics	Tukysa	2020	ErbB2/HER2	HER2-positive breast cancer and colon cancer
Upadacitinib	ABT-494	AbbVie	Rinvoq	2019	JAK1	Second-line treatment for rheumatoid arthritis, psoriatic arthritis, atopic dermatitis
Vandetanib	ZD6474	Sanofi	Zactima	2011	VEGFR2	Medullary thyroid cancer
Vemurafenib	PLX-4032	Genentech	Zelboraf	2011	BRAF	*BRAF V600E* or *V600K* mutation positive melanoma with cobimetinib; Chester-Erdheim disease
Zanubrutinib	BGB3111	BeiGene	Brukinsa	2019	BTK	Mantle cell lymphoma

[a] Data from Refs. [10–13].
[b] Although many of these drugs are multikinase inhibitors, only the primary therapeutic targets are given here.
[c] AML, acute myelogenous leukemia; CML, chronic myelogenous leukemia; ErbB2/HER2, human epidermal growth factor receptor-2; MET (HGFR), hepatocyte growth factor receptor; NSCLC, non-small cell lung cancer; Ph^+, Philadelphia chromosome-positive; RCC, renal cell carcinoma.

(DDR1) and receptor-2 (DDR2). DDR1/2, which are activated by collagen, participate in cell proliferation, differentiation, migration, and remodeling the extracellular matrix. Imatinib is FDA-approved for (i) the first-line treatment of Philadelphia chromosome-positive chronic myelogenous leukemia, (ii) *KIT* mutation-positive gastrointestinal stromal tumors, (iii) myelodysplastic/myeloproliferative diseases with *PDGFR* gene-rearrangements, (iv) acute lymphoblastic leukemia, (v) chronic eosinophilic leukemia, (vi) hypereosinophilic syndrome, (vii) dermatofibrosarcoma protuberans, and (viii) as a second-line treatment for aggressive systemic mastocytosis without the KIT^{D816V} mutation [2, 10]. Furthermore, imatinib is used off-label for the treatment of chordomas, advanced *KIT*-mutant melanomas, desmoid tumors, and chronic myelogenous leukemia following allogeneic stem cell transplantation. Imatinib is thus a broad-spectrum inhibitor.

2. Protein kinase structure and mechanism

2.1. Primary, secondary, and tertiary structures

The newly approved drugs described in this review interact with (i) the protein-serine/threonine kinase PKB – also known as AKT, (ii) the VEGF, Flt3, ROS1 receptor protein-tyrosines, and the nonreceptor protein tyrosine kinases JAK1/2/3 and BTK so that the following description is generic. As described originally for PKA (protein kinase A) by Knighton et al., protein kinases have a small amino-terminal lobe and large carboxyterminal lobe (Fig. 1A) [18]. The small lobe is made up of a five-stranded antiparallel β-sheet (β1–β5) and an αC-helix that occurs in active and inactive orientations (Fig. 1C) [19,20]. The small lobe contains a glycine-rich loop (GRL), sometimes called the P-loop (for the ATP phosphates), which connects the β1- and β2-strands of the N-terminal lobe; the loop consists of GxGxΦG where the Φ denotes a hydrophobic residue. A valine residue that is two residues after the G-rich loop makes hydrophobic contact with the adenine base of ATP as well as numerous small molecule protein kinase antagonists. Protein kinase enzymes contain an AxK sequence within the small lobe β3-strand and a conserved glutamate near the middle of the αC-helix. A salt bridge connects the positively charged β3-strand lysine (K) and the negatively charged αC-glutamate (E) in active protein kinases and such structures correspond to an "αC_{in}" conformation (Fig. 1A and C). The αC_{in} architecture is necessary, but not sufficient, for the manifestation of full enzyme activity. Furthermore, the absence of this salt bridge indicates that the enzyme is catalytically inactive and the corresponding structure corresponds to the "αC_{out}" conformation (Fig. 1E). Note that the lysine and glutamate in Fig. 1E structure are too far apart to form a salt bridge, but the distance between lysine and glutamate in most αC_{out} structures is about twice that depicted here. The conversion of the αC_{out} to the αC_{in} conformation is required for catalytic activity.

The large lobe is mainly α-helical (Fig. 1C) with eight conserved helices (αD–αI, αEF1, αEF2) [21], not all of which are shown in this two-dimensional rendering. The carboxyterminal lobe of catalytically active protein kinases also contains four short β-strands (β6–β9) (Fig. 1A shows only the β7- and β8-strands). The second residue of the β7-strand is the floor of the adenine binding pocket, and this residue interacts hydrophobically with all known ATP-competitive protein kinase inhibitors [22]. The carboxyterminal lobe contains a catalytic loop (CL) that mediates the transfer of the γ-phosphoryl group from ATP to the protein substrates. The C-terminal lobe also positions the protein substrate into the active site to enable catalysis.

Hanks and Hunter described 12 subdomains (I–VIa, VIb–XI) that make up the functional components of protein kinases [23]. A K/E/D/D (Lys/Glu/Asp/Asp) tetrad plays an essential role in the enzymatic activity of all protein kinases. The *K* of the tetrad is the β3-strand lysine that forms salt bridges with the (i) αC-glutamate to form the αC_{in} structure and the (ii) α-phosphate and (iii) β-phosphate of ATP (not shown). Residues within the kinase activation segment position the

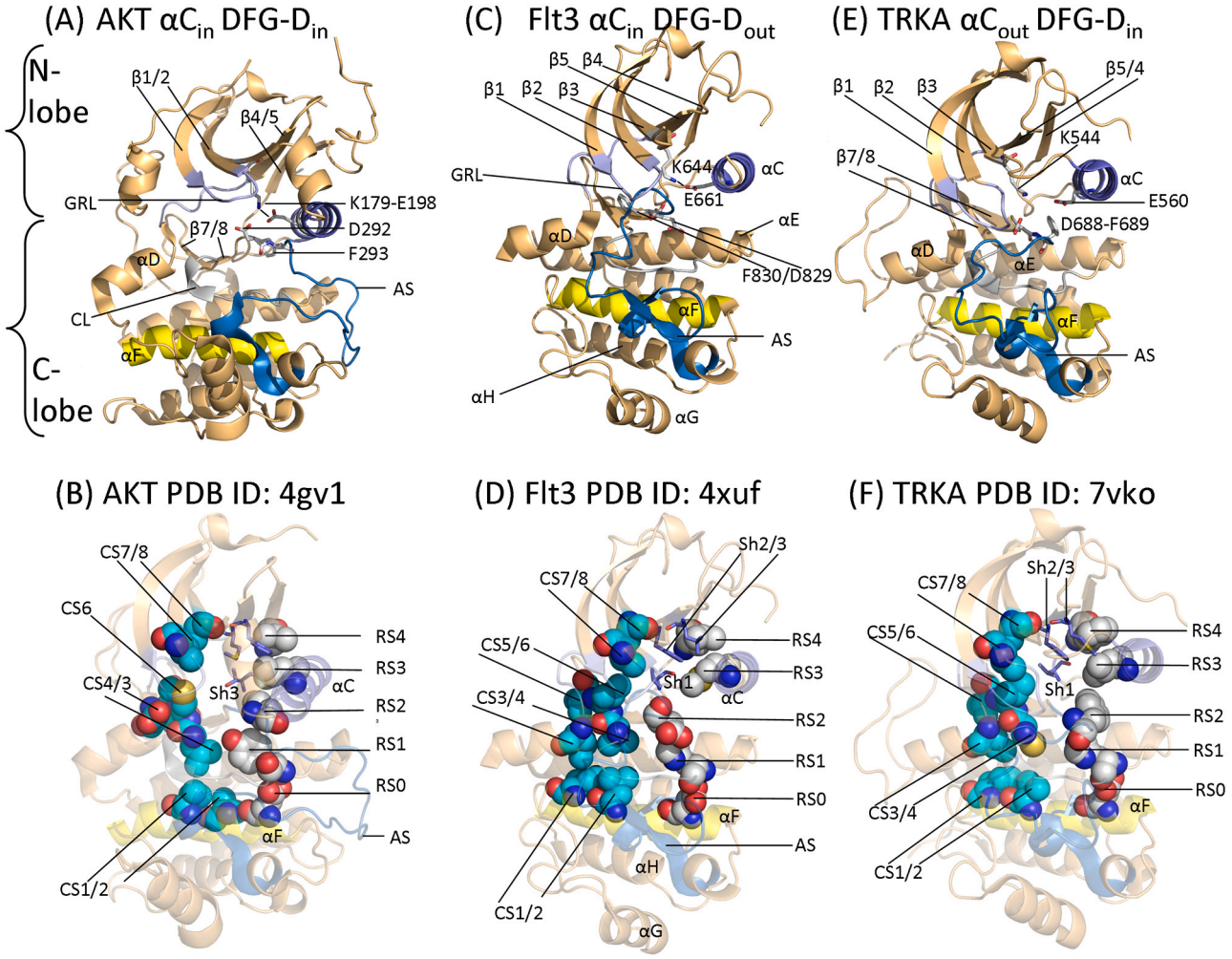

Fig. 1. (A) Overview of active AKT/PKB and (B) its C-spine and R-spine residues – CS5 is hidden. (C) The αC_{in} and DFG-D_{out} structure of dormant Flt3 and (D) its C-spine, R-spine, and shell residues. (E) Overview of the αC_{out} DGF-D_{in} structure of TRKA and (F) its C-spine and R-spine residues. AS, activation segment; CL, catalytic loop. GRL, glycine-rich loop. Figs. 1, 2 C, and 5 were prepared using the PyMOL Molecular Graphics System Version 1.5.0.4 Schrödinger, LLC.

phosphorylatable substrate into the active site. Moreover, the HRD-D of the catalytic-loop (the first *D* of the K/E/*D*/D tetrad) functions as a Lowry-Brönsted base (proton acceptor). Madhusudan et al. suggested that the HRD-D of the catalytic loop abstracts the proton from the protein substrate –OH [24]. Furthermore, Zhou and Adams hypothesized that the HRD-D positions the protein substrate hydroxyl group to facilitate the in-line nucleophilic attack of the oxygen with the γ-phosphate of ATP [25]. See Ref. [26] for a comprehensive summary of protein kinase enzymology and see Table 3 for an inventory of the important residues of four of the protein kinases considered in this article.

The second *D* of the K/E/D/*D* tetrad is the first residue of the protein-substrate-binding activation segment. This component of all protein kinases starts with DFG and ends with APE or a similar triad such as PPE. Activation segments, which are about 35–40 residues long, are important regulatory and structural components of all protein kinases [27]. An HRD(x)$_4$N signature makes up the catalytic loop of functional protein kinases. The activation segment occurs carboxyterminal to the catalytic loop. Two Mg^{2+} ions – Mg^{2+}(1) and Mg^{2+}(2) – are required for the activity of most, but not all, protein kinases. Mg^{2+}(1) bonds with the activation segment DFG-D and Mg^{2+}(2) bonds with the terminal catalytic loop asparagine (not shown).

The amino acid sequence and length of the middle portion of the activation segment vary greatly within the protein kinase superfamily [2]. The activation segment of nearly all protein kinases contains one or more phosphorylatable residues. Moreover, activation segment phosphorylation is necessary for the expression of maximal enzyme activity in nearly all protein kinases. ErbB1/2/4 of the EGFR family and Flt3 represent notable exceptions because they exhibit maximal activity without activation segment phosphorylation. The protein kinase activation segment DFG occurs spatially near the conserved catalytic loop HRD sequence and the αC-helix. The regulatory αC-helix, which occurs within the small lobe, nevertheless occupies a strategically important location between the two lobes. The protein kinase activation segment has an open and extended structure in the functional form of all protein kinases (Fig. 1A) and a closed structure in most inactive kinases (Fig. 1C/E) [2]. The first two activation segment residues occur in different conformations. The DFG-D side chain of active protein kinases points inward toward the ATP-binding site and it binds Mg^{2+}(1). This structure is known as the "DFG-D_{in}" conformation (Fig. 1A/E). The DFG-D side chain in many inactive protein kinases points away from the ATP-binding site. This structure is known as the "DFG-D_{out}" conformation (Fig. 1C). It is the ability of DFG-D to bind (DFG-D_{in}) or not bind (DFG-D_{out}) Mg^{2+}(1) within the active site that is significant.

Modi and Dunbrack investigated the interaction of ligands and drugs with active and inactive conformations of protein kinases based upon the structure of the activation segment, which begins with the canonical DFG sequence [28,29]. As noted, this triad is seen in two major conformations: DFG-D_{in} and DFG-D_{out}. In the first case, the phenylalanine residue interacts with the αC-helix of the small lobe and in the second case the phenylalanine is found in a portion of the physiological ATP site thereby creating an αC-helix pocket. These authors found a constellation of protein kinase structures that depend upon the location of the phenylalanine side chain (DFG-D_{in}, DFG-D_{out}, and DFG-$D_{intermediate}$) and the backbone dihedral angles of the xDF sequence where x is the residue before the DFG signature. They identified eight different configurations and classified them based upon the conformation (χ1) of the phenylalanine rotamer (minus, plus, trans) and on the Ramachandran regions (A, alpha; B, beta; L, left) of the xDF motif. Their clusters divide the DFG-D_{in} configuration into six groups including BLAminus, which corresponds to active structures, and two common inactive forms, ABAminus and BLBplus. DFG-D_{out} structures occur principally in the BBAminus conformation. The inactive structures possess features that block their interaction with Mg^{2+}, ATP, and/or their protein substrates. Modi and Dunbrack established a valuable searchable and noncommercial web site (http://dunbrack3.fccc.edu/kincore/) that lets one determine whether a protein kinase conformation corresponds to an active enzyme or to an inactive enzyme. We used this web site to decide whether the structures of our various drug-enzyme complexes correspond to active (DFG-D_{in}, BLAminus) or dormant (otherwise) enzymes.

2.2. Protein kinase hydrophobic skeletons and shell residues

Kornev et al. analyzed the three-dimensional structures of about two dozen protein kinases to identify structurally and functionally important residues [30,31]. Their studies revealed a quartet of four amino acids that make up an R-spine (regulatory spine) and an octet of eight amino acids along with the adenine base of ATP that make up a C-spine (catalytic spine). These residues occur in both the small and large lobes. These spines produce a stable, but flexible, catalytically active ensemble. The C-spine positions ATP and the R-spine positions the protein substrate for catalysis. The R-spine contains components from both the αC-helix and the activation segment, whose structures are important in determining active and dormant enzyme states. The exact positioning and alignment of both spines are necessary, but not sufficient, for the formation of catalytically competent protein kinases.

The R-spine contains the first residue of the β4-strand and the amino acid that is four residues C-terminal to the conserved αC-helix glutamate, both of which are within the small lobe [30]. The R-spine also contains the DFG-Phe of the activation segment and the HRD-His of the catalytic loop, both within the large lobe. The HRD-His N–H backbone

Table 3
Important residues in selected human protein kinases.

	AKT	BTK	Flt3	TRKA
Number of residues	480	659	993	796
Signal peptide	None	None	1–26	1–32
Extracellular segment	None	None	27–543	33–423
Transmembrane segment	None	None	544–563	424–439
Intracellular portion	1–480	1 – 659	564–993	440–796
Protein kinase domain	143–408	402–655	610–943	510–781
Glycine-rich loop	^{157}GKGTFG^{162}	^{409}GTGQFG^{414}	^{167}GSGAFG^{622}	^{577}GEGAFG^{522}
The β3-*K* of K/*E*/D/D	K189	K430	K644	K544
αC-*E* of K/*E*/D/D	E198	E475	E661	E560
Hinge-linker residues	^{46}EYANGGE^{52}	^{475}EYMANG^{480}	^{692}EYCCYGD^{698}	^{590}EYMRHGD^{596}
Gatekeeper residue	M45	T474	F691	F589
Catalytic Y/HR*D* residue, the first *D* of K/E/*D*/D	D274	D521	D811	
Catalytic loop	^{272}YRDLKLEN^{279}	^{519}HRDLAARN^{526}	^{809}HRDLAARN^{816}	^{648}HRDLATRN^{655}
AS[a] *D*FG, the second *D* of K/E/D/*D*	D292	D539	D829	D688
AS[a] threonine/tyrosine phosphorylation site	T308	Y551	Y842	Y676/680/681
End of the AS[a]	^{317}APE^{319}	^{565}PPE^{567}	^{856}APE^{858}	^{695}PPE^{697}
Molecular weight (kDa)	55.7	76.3	112.9	87.5
UniProtKB ID	P31749	Q06187	P36888	PO4629

[a] AS, activation segment.

hydrogen bonds with the side chain of a conserved aspartate within the hydrophobic αF-helix. From the base to the apex, Meharena et al. labeled the R-spine residues as RS0, RS1, RS2, RS3, and RS4 [32]. We later labeled the C-spine residues from the bottom to the top as residues CS1–8 (Fig. 1B/D/F) [33]. We observed that the R- and C-spines of active protein kinases are linear (Fig. 1B). In kinases with the DFG-D_{out} structure, the DFG-D residue (RS2) is displaced toward the left and the R-spine is broken (Fig. 1D). RS3 is displaced toward the right in protein kinases with the αC_{out} structure (Fig. 1F). The identity of the R-spine, C-spine, and shell residues of four of the protein kinases considered in this article are provided in Table 4.

The location of the protein kinase spine and shell residues plays an important role in determining the activity of these enzymes; one cannot overemphasize their significance in supporting the activity of this enzyme family as well as their participation in their interactions with small molecule protein kinase blockers. For a summary of the properties of the spine and shell residues and their interactions with low molecular weight inhibitors of important members of the protein kinase family, see the following articles: Refs. [34–36] for the ALK midkine and pleotrophin receptor protein-tyrosine kinase, Refs. [16,37–39] for the EGFR family (ErbB1/2/3/4) of protein-tyrosine kinases, Ref. [40] for the protein-tyrosine kinases of the PDGFRα/β group, Ref. [41] for protein-tyrosine kinases of the fibroblast growth factor receptor family, Ref. [42] for the protein-tyrosine kinase corresponding to the Kit stem cell receptor, Ref. [43] for the RET glial-cell derived receptor protein-tyrosine kinase, Ref. [44] for the protein-tyrosine kinases of the VEGFR1/2/3 family, Ref. [45] for the ROS1 orphan receptor protein-tyrosine kinase, Ref. [46] for the protein-tyrosine kinase corresponding to the Flt3 receptor, Refs. [22,47] for the nonreceptor BCR-Abl protein tyrosine kinase, Ref. [48,49] for the nonreceptor Janus protein-tyrosine kinases, Refs. [16,50] for the nonreceptor Bruton protein-tyrosine kinase, Refs. [51,52] for the nonreceptor Src protein-tyrosine kinase, Refs. [53,54] for the dual specificity MEK1/2 protein kinases, Refs. [21,55] for the CDK4/6 protein-serine/threonine kinases, Refs. [56,57] for the ERK1/2 protein-serine/threonine kinases, Refs. [58,59] for the RAF protein-serine/threonine kinases, and Ref. [9] for phosphatidylinositol 3-kinase (PI3K), a member of the atypical protein kinase group.

The catalytic spines of protein kinases consist of two residues from the N-lobe and six residues from the C-lobe. The adenine base of ATP connects these two parts of the C-spine and this process enables the functional merging of the two lobes of the enzyme and promotes catalysis [31]. The two small lobe residues that bind to the adenine moiety of ATP include the conserved β2-strand valine (CS7) after the glycine-rich loop and the conserved β3-strand alanine (CS8) of the AxK motif. A hydrophobic amino acid side chain from the middle of the carboxyterminal lobe β7-strand (CS6) interacts with the adenine moiety of ATP. Moreover, the β-7 strand CS4 and CS5 residues interact with CS3 at the proximal portion of the αD-helix. Additionally, CS3 makes hydrophobic contact with (i) the neighboring CS4 and (ii) CS1 within the αF-helix below it. Both the R- and C-spines interact with the hydrophobic αF-helix below them; the αF-helix contains CS1, CS2, and RS0 and it serves as a major foundation that stabilizes and supports the entire protein kinase domain (Fig. 1D). The protein kinase hinge and linker residues connect the two protein kinase lobes and the 6-amino N–H group of ATP hydrogen bonds with the backbone carbonyl group of the first hinge residue (not shown). Also, the *N*1 of the adenine group of ATP forms a hydrogen bond with the backbone N–H group of the third hinge residue (not shown). Almost all ATP small-molecule steady-state competitive protein kinase blockers form a hydrogen bond with backbone hinge residues, most commonly with that of the third hinge residue [33].

Based upon site-directed mutagenesis experiments, Meharena et al. found three residues in murine protein kinase A that strengthen and stabilize the regulatory spine, which they labeled as Sh1, Sh2, and Sh3 where Sh refers to shell [32]. Their Sh1 mutant (V104G) had 5% of the activity of the wildtype enzyme and their Sh2/Sh3 double mutant (M120G/M118G) was devoid of all catalytic activity. These findings demonstrate that the shell residues support PKA activity. We hypothesize that the corresponding shell residues play a related stabilizing function for all protein kinases. The Sh1 residue occurs within the segment connecting the αC-helix with the β4-strand, the so-called back loop. The Sh2 residue (the gatekeeper) occurs at the end of the β5-strand proximal to the hinge segment and the Sh3 residue is found two residues upstream from the Sh2 residue within the β5-strand.

The term gatekeeper refers to the function that this residue plays in controlling access to the hydrophobic pocket adjoining the adenine binding pocket [60,61], a residue that consistently interacts with many small molecule protein kinase antagonists. A large amount of data indicate that many small molecule therapeutic steady-state ATP-competitive protein kinase inhibitors interact with the R-spine (RS2/3), the C-spine (CS6/7/8), and shell (Sh1 and Sh2) residues. Ung et al. reported that about three-quarters of protein kinases have a relatively large gatekeeper residue (e.g., Met, Leu, Phe) while about one-quarter have smaller gatekeeper residues (e.g., Thr, Val) [62]. Also of importance in long-term drug effectiveness, the gatekeeper residue of targeted protein kinases is one of the more common sites of drug-resistant mutations [3,63].

Table 4
Spine and shell residues of selected human protein kinases [a].

	Symbol	Klifs No.	AKT	BTK	Flt3	TRKA
Regulatory spine						
β4-strand (N-lobe)	RS4	38	L213	L460	L677	F575
C-helix (N-lobe)	RS3	28	L202	M449	M665	L654
Activation loop DFG-F (C-lobe)	RS2	82	F293	F540	F830	F669
Catalytic loop HRD-H (C-lobe)	RS1	68	Y272	H519	H809	H648
F-helix (C-lobe)	RS0	None	D331	D579	D870	D709
Shell						
Two residues upstream from the gatekeeper	Sh3	43	F225	I472	L689	M587
Gatekeeper, end of β5-strand	Sh2	45	M227	T474	F691	F589
αC-β4 loop	Sh1	36	T211	V458	V675	V573
Catalytic spine						
β3-AxK-A (N-lobe)	CS8	15	A177	A428	A642	A542
β2-strand (N-lobe)	CS7	11	V164	V416	V624	V524
β7-strand (C-lobe)	CS6	77	M281	L528	L818	L657
β7-strand (C-lobe)	CS5	78	L282	V529	V819	V658
β7-strand (C-lobe)	CS4	76	L280	C527	V817	C656
D-helix (C-lobe)	CS3	53	E234	L482	L699	L597
F-helix (C-lobe)	CS2	None	L334	L586	L877	V716
F-helix (C-lobe)	CS1	None	V338	L590	I881	I720

[a] From Ref. [30–32], https://klifs.net/, and https://www.uniprot.org/uniprotkb/.

3. A classification of protein kinase-inhibitor complexes and a description of inhibitor-binding pockets

Based upon earlier reports [61,64–67], we classified the small molecule protein kinase inhibitors into seven main groups including reversible (Groups I, I½, II, III, IV, and V) and targeted covalent irreversible inhibitors (VI) as noted in Table 5. We divided the type I½ and type II antagonists into A and B subtypes [33]. Subtype A drugs extend past the gatekeeper residue into the back cleft. Contrarywise, subtype B drugs do not extend into the back cleft. The possible significance of this difference, based on incomplete data, is that subtype A antagonists bind to their enzyme target with longer residence times when compared with subtype B blockers [33]. For example, sorafenib is a type IIA VEGFR inhibitor and sunitinib is a type IIB VEGFR antagonist, both of which are FDA-approved for the treatment of renal cell carcinoma. The type IIA blocker has a residence time greater than 64 min while the type IIB

Table 5
Classification of small molecule protein kinase inhibitors [a].

Inhibitor type	Properties
I	Binds in and around the ATP-binding pocket of an active enzyme
I½ A/B	Binds in and around the ATP-binding pocket of an inactive DFG-D_{in} enzyme
I½ A	Extends into the back cleft
I½ B	Does not extend into the back cleft
II A/B	Bind in and around the ATP-binding site of an inactive DFG-D_{out} enzyme
II A	Extends into the back cleft
II B	Does not extend into the back cleft
III	Allosteric inhibitor bound next to the ATP-binding site
IV	Allosteric inhibitor bound away from the ATP-binding site
V	Bivalent inhibitor spanning two kinase domain regions
VI	Covalent inhibitor

[a] Ref. [33].

Table 6
Location of important residues within the front cleft, gate area, and back cleft.

Description	Location	KLIFS residue no[a]
GxGxΦG	Front cleft	4–9
β2-strand V (CS7)	Front cleft	11
β3-strand A (CS8)	Front cleft	15
HRD with DFG-D_{in}	Front cleft	68–70
$HRD(x)_4N$-N	Front cleft	75
β7-strand CS6	Front cleft	77
β3-strand K	Gate area	17
αC-β4 penultimate back loop residue	Gate area	36
Gatekeeper	Gate area	45
The x of xDFG	Gate area	80
DFG	Gate area	81–83
αC-helix E	Gate area	24
RS3	Gate area	28
β4/β5-strands	Back cleft	38-44
αC-helix	Back cleft	20-30
αE-helix	Back cleft	60-64
HRD with DFG-D_{out}	Back cleft	68–70

[a] Refs. [69,70].

inhibitor has a residence time of less than 2.9 min [33].

We followed the work of Liao, van Linden et al., Kooistra et al., and Kanev et al. [67–70] in describing and distinguishing drug-binding pockets. A summary depicting the location of the pockets and sub-pockets is provided in Fig. 2 as described in Table 6. The topography between the N- and C-terminal protein kinase lobes is divided into a front cleft or pocket, a gate area, and a back cleft. The back pocket (hydrophobic pocket II, or HPII) includes the gate area and the bordering back cleft. The front cleft contains the hinge residues, the linker residues that connect the hinge residues to the αD-helix in the large lobe, the glycine-rich loop, the adenine-binding pocket (AP), and the catalytic loop ($HRD(x)_4N$).

Type I inhibitors bind within the front cleft. The gate area includes residues from both lobes. The gate area contains the last three residues of the β3-strand and the first two residues of the following β3-αC loop. It also includes the residue directly before the activation segment (the x of xDFG) along with the first five residues of the activation segment. The back cleft includes the middle residues of the αC-helix, the entire β4-strand, and the entire β5-strand. The back cleft also contains the entire αE-helix and the three residues before the catalytic loop HRD. Several type I½ inhibitors are found in both the front cleft and a portion of the back cleft. One of the general goals in the design of small molecule protein kinase blockers is to maximize selectivity and to minimize off-target side effects [65]; this approach can be facilitated by comparing drug interactions with target and nontarget kinases [71–73]. Producing ligand fragments that bind to residues that border the various pockets plays a strategic role in protein kinase antagonist development with the objective of maximizing drug affinity.

van Linden et al. [68] and Kanev et al. [70] described ligand and drug binding to more than 5200 human and mouse protein kinases. Their KLIFS (kinase–ligand interaction fingerprint and structure) collection includes an alignment of 85 ligand binding-site residues that occur in both lobes; their summary aids in the evaluation of ligands and drugs based upon their binding properties. Such data help in the recognition of common and unique drug-enzyme interactions. These authors formulated a standard amino acid residue numbering system that aids in the comparison of different protein kinases and their ligands. Table 4 depicts the relationship of the KLIFS database nomenclature and the C-spine, R-spine, and shell amino acid residue numbering system and Fig. 3 depicts the location of the KLIFS residues within the protein kinase domain. Moreover, these authors produced a valuable searchable and noncommercial web site that is regularly updated that provides comprehensive information on the interaction of protein kinases with drugs and ligands (klifs.net).

In addition, Carles et al. released a complete listing of protein kinase antagonists that are in clinical trials or that have been approved by various regulatory agencies [6]. They posted a searchable and noncommercial web site that is regularly updated that depicts the structure and physical properties of the various drugs, their protein kinase targets, therapeutic indications and trade names, and the year of first approval by regulatory agencies (if applicable) (http://www.icoa.

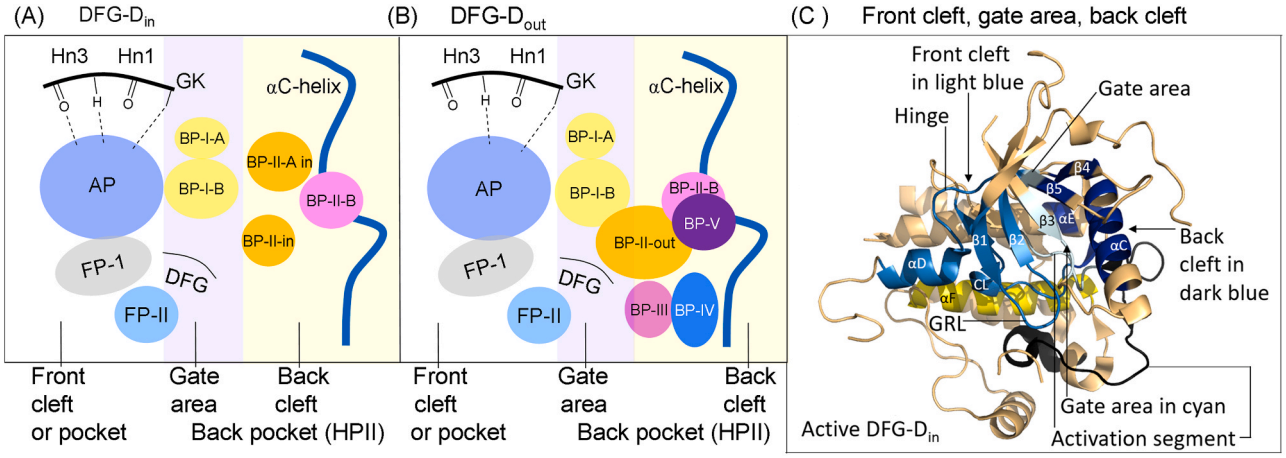

Fig. 2. (A) Location of the protein kinase domain drug-binding pockets in the DFG-D_{in} enzyme form. (B) Location of the drug-binding pockets in the DFG-D_{out} enzyme form. Adapted from Refs. [67–69]. (C) Location of the protein kinase front cleft, gate area, and back cleft. AP, adenine pocket; BP, back pocket; FP, front pocket; Hn, hinge; HPII, hydrophobic pocket II; GK, gatekeeper.

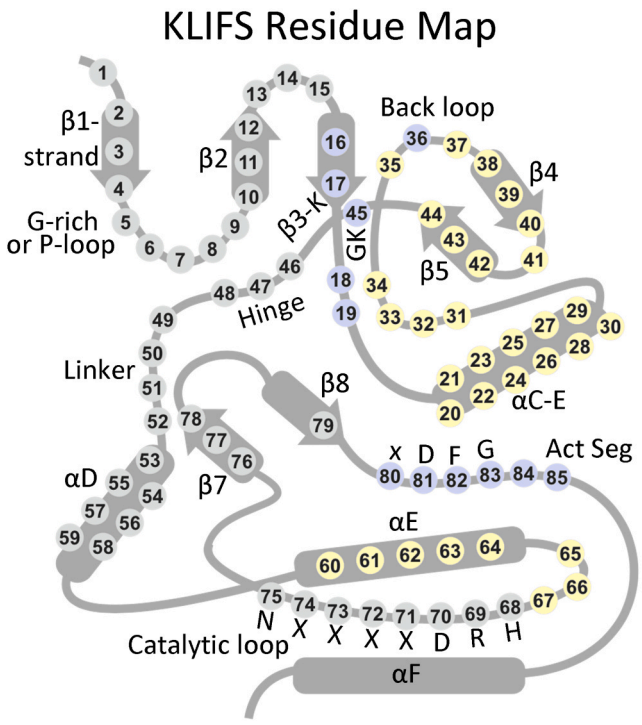

Fig. 3. The location of the KLIFS residues within a generic protein kinase domain. Act Seg, activation segment. Residues in gray circles are found in the front cleft; blue circles, gate area; yellow circles, back cleft.

fr/pkidb/). Likewise, the Blue Ridge Institute for Medical Research (BRIMR) maintains a web site that lists the FDA-approved protein kinase antagonists and provides their (i) molecular structures, (ii) the number of hydrogen bond donors/acceptors, (iii) the calculated Log of the partition and distribution coefficients, (iv) the number of rings and rotatable bonds, (v) the year of initial approval, (vi) their primary protein kinase targets, (vii) and their therapeutic indications. The website also provides a link to the corresponding FDA labels. This website (www.brimr.org/PKI/PKIs.htm) is updated following FDA-approval of new protein kinase antagonists.

4. Drug-enzyme interactions: capivasertib, pirtobrutinib, quizartinib, repotrectinib

4.1. Capivasertib and AKT

The phosphatidylinositol 3-kinase (PI3K)/AKT/mammalian target of the rapamycin (mTOR) pathway is involved in various crucial cellular functions such as growth, proliferation, metabolism, and survival [74]. Activation of this signaling pathway is triggered by receptor protein-tyrosine kinases and G protein-coupled receptors located in the plasma membrane, which promote the recruitment of class I PI3K by adaptor proteins, such as the insulin receptor substrate (IRS). This leads to the conversion of phosphatidylinositol 4,5-bisphosphate (PIP_2) to phosphatidylinositol 3,4,5-trisphosphate (PIP_3) as the phosphoryl group is added to the 3' position of the inositol ring. PIP_3 functions as a second messenger that recruits and activates AKT, which in turn catalyzes the phosphorylation and inactivation of tuberous sclerosis complex (TSC) 1/2, negative regulators of mTORC1 (mammalian target of rapamycin complex-1). Colocalization of AKT with 3-phosphoinositide-dependent protein kinase 1 (PDK1) at the plasma membrane permits the phosphorylation of AKT T308 within its activation segment leading to enhanced enzyme activity. Finally, activation of mTORC1 induces S6- and 4E-BP1-mediated protein synthesis and decreased autophagy, resulting in cell growth and proliferation. The downstream effects of PI3K activation can be antagonized by the tumor suppressor phosphatase and tensin homolog (PTEN) by the dephosphorylation of PIP_3 back to PIP_2.

The AKT family consists of AKT, AKT2, and AKT3. These three enzymes, which belong to the ACG protein kinase family (PKA, PKC, and PKG), possess an N-terminal pleckstrin homology (PH) domain, a central protein-serine/threonine kinase domain, and a short C-terminal regulatory domain [75]. Of the members of the ACG family, AKT, AKT2, AKT3, P70S6K and PKA had low nanomolar capivasertib IC_{50} values. In contrast, the closely related ROCK2 along with MKK1, MSK1/2, PKCα/β/δ/η/θ, PKGα/β, PRKX, RSK2/3, and P70S6K had higher capivasertib IC_{50} values.

The frequent activation of the PI3K/AKT/mTOR pathway and its crucial role in the pathogenesis of estrogen receptor-positive (ER^+) breast cancer has made it an attractive therapeutic target in this breast cancer subtype. Consequently, the number of new antagonists in clinical development targeting this pathway has greatly increased. Among these, the pan-AKT inhibitor capivasertib was approved in 2023 in combination with the estrogen receptor degrader fulvestrant for the treatment of ER^+ advanced breast cancer after progression on an aromatase inhibitor. However, the clinical development of multiple inhibitors of the PI3K/AKT/mTOR pathway, in parallel with the incorporation of CDK4/6 inhibitors into the standard of care of ER^+ advanced breast cancer, has led to a multitude of available therapeutic regimens and many possible combined therapeutic strategies for the treatment of this disorder.

Capivasertib is a pyrrolo[2,3-*d*]pyrimidine derivative (Fig. 4A) that is FDA-approved for the treatment of HR^+-HER2-negative breast cancer (Table 2). Addie et al. determined the X-ray crystal structure of capivasertib bound to AKT and they observed that the pyrrolopyrimidine ring forms hydrogen bonds with hinge residues E228 and A230 (Fig. 5A) [75]. Moreover, the central piperidine ring adopts an axial conformation with respect to both the pyrrolopyrimidine hinge group and the GRL aryl group. This axial over equatorial preference is influenced by the ortho-sp^2 nitrogen in the pyrrolopyrimidine core and the adoption of this conformation positions the basic amino group in the acidic hole formed by E234 and E278 and the p-chlorophenyl group in a hydrophobic pocket under the GRL formed by the side chains of K179, L181, and V164 and the backbone atoms of K158 and G162. Capivasertib makes hydrophobic contact with the gatekeeper residue (M227) and CS6/7/8 (M281, V164, A177). Modi and Dunbrack found that this enzyme occurs within the active BLAminus enzyme cluster, and they classify capivasertib as a type I inhibitor [29]. The drug occupies the front pocket and FP-II and of an active enzyme (BLAminus) and we also classify it as a type I inhibitor [33]. See Ref. [74] for the results of the clinical trials that led to the approval of capivasertib in the United States in 2023.

4.2. Pirtobrutinib and BTK

The Bruton kinase (BTK) was originally identified in 1993 as a nonreceptor protein-tyrosine kinase that is defective in X-linked agammaglobulinemia [76]. B lymphocytes and immunoglobulins are almost completely lacking in affected males with this rare affliction making them susceptible to infections, but they respond favorably to parenteral injections of human immunoglobulins [77]. People with this malady have no significant alterations in cells other than B cells, and this finding is in accord with the restriction of clinical features to B cell function. During development, each B cell recombines immunoglobulin variable (V), diversity (D), and junction genes (J) thereby forming a unique sequence that establishes the antigen-binding site of the B cell receptor [50]. Signaling from this receptor requires a network of protein kinases and adaptor proteins that convert antigenic stimulation to intracellular responses. The B cell receptor complex consists of the receptor linked to an Igα-Igβ heterodimer with disulfide bonds. After antigenic stimulation of the receptor, the Src family kinase Lyn mediates the phosphorylation of pairs of tyrosine residues in Igα-Igβ immunoreceptor tyrosine-based

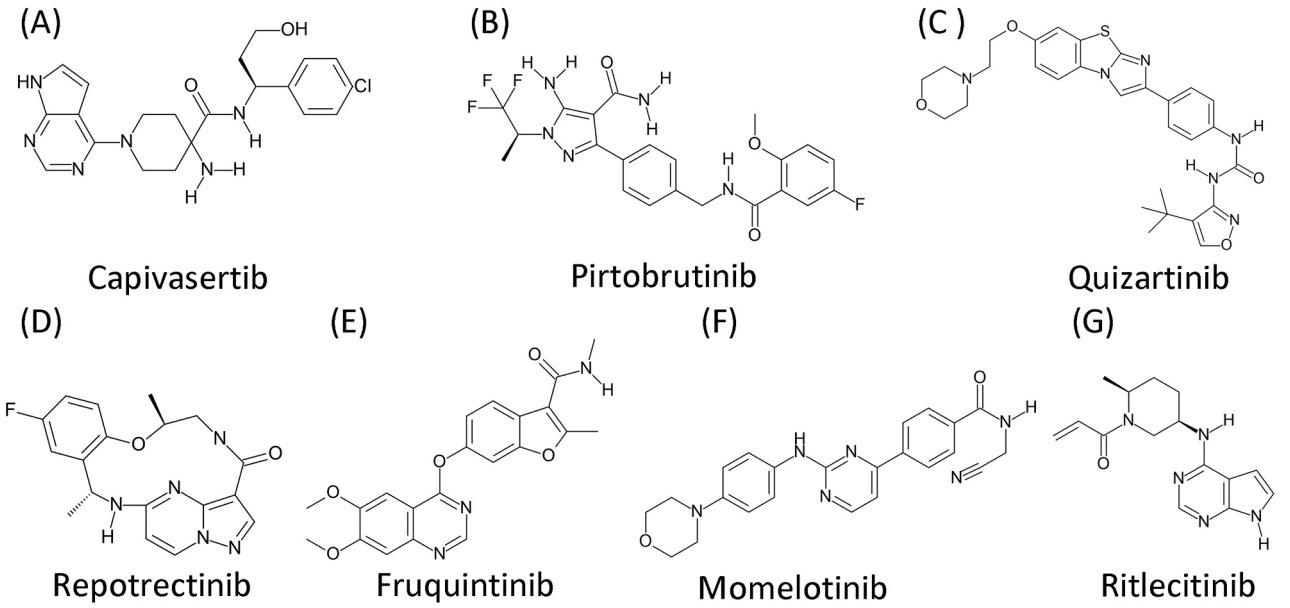

Fig. 4. (A–G). Chemical structures of selected FDA-approved protein kinase antagonists.

activation motifs (ITAMs) thus creating a docking site for the two SH2 domains of SYK (spleen tyrosine kinase). SYK attracts and activates PI3K-δ, which catalyzes the conversion of membrane-associated phosphatidylinositol 4,5 bisphosphate (PIP_2) to phosphatidylinositol 3,4, 5-trisphosphate (PIP_3). The N-terminal PH (Pleckstrin Homology) lipid-interaction module of BTK is attracted to PIP_3 thereby allowing SYK and Lyn to catalyze the trans-phosphorylation of BTK at Y551 within the activation segment and this phosphorylation results in enzyme activation.

BTK catalyzes the phosphorylation of PLCγ2 at residues Y753 and Y759 to produce an increase in phospholipase activity [50]. PLCγ2 mediates the hydrolysis of PIP_2 to generate inositol trisphosphate (IP_3) and diacylglycerol (DAG). IP_3 releases Ca^{2+} from intracellular stores, which activates PLCγ2. In turn, DAG and Ca^{2+} activate PKCβ, which leads to the activation of the RAS-RAF-MEK-ERK signaling module that promotes cell growth and proliferation. PKCβ also activates the NF-κB pathway. IκBα (inhibitor of kappa B-α) disables the NF-κB transcription factor by masking the nuclear localization signals of NF-κB and keeps it sequestered in an inactive state in the cytoplasm. The inhibitor of κB kinase (IKK) mediates the phosphorylation of the inhibitory IκBα, which results in its (i) dissociation from NF-κB, (ii) ubiquitylation, and (iii) proteosomal degradation. The unsequestered NF-κB translocates into the nucleus and activates the expression of more than 150 genes. NF-κB is a rapidly acting transcription factor that regulates, inter alia, cell survival and cytokine production. As a result of BTK inhibition, B cells may be released from lymphatic tissue into the blood stream, which is commonly observed after treatment of patients with BTK antagonists. An increase in B cell antigen receptor signaling occurs in various B cell lymphomas. Many lymphomas maintain B cell receptor signaling by responding to self antigens within the tumor microenvironment and B cell proliferation that is driven by self antigens is essential for the pathogenesis of these afflictions.

BTK belongs to the TEC family of nonreceptor protein-tyrosine kinases that includes BTK, TEC, ITK (inducible T cell kinase), TXK (also known as RLK, resting lymphocyte kinase), and BMX (bone marrow-expressed kinase) [50]. BTK and other TEC family kinases contain a short N-terminal pleckstrin homology (PH) domain, a TEC homology (TH) domain, followed by an SH3, SH2, and C-terminal protein kinase domain. The PH domain of the TEC family is attracted to membrane-associated PIP_3, which is responsible for membrane-localization. Following B cell receptor activation of PI3K and the generation of PIP_3, the canonical PIP_3-binding site in the PH-TH module is attracted to the plasma membrane by a process that disrupts the compact inactive conformation. The association of two enzyme molecules leads to the trans-phosphorylation of Y551 within the activation segment of one or both proteins thereby leading to the activated state. Activated BTK can then participate in the signal transduction module involving PLCγ2, PKCβ, RAS-RAF-MEK-ERK, and NF-κB.

People with mantle cell lymphoma, which makes up about 6% of non-Hodgkin lymphomas, usually present with palpable lymphadenopathy at a median age of about 65 years [50]. The male/female ratio is 4/1. Nearly 70% of patients are at stage IV at the time of diagnosis with peripheral blood, bone marrow, spleen, and gastrointestinal involvement. The historical median overall survival in people with newly diagnosed mantle cell lymphoma was three to four years. These B cell lymphomas have a t(11:14) (q13:q32) chromosomal translocation between the immunoglobulin heavy chain gene on chromosome 14 and the *CCND1* gene on chromosome 11, which leads to the constitutive overexpression of cyclin D1. Cyclin D1 activates CDK4 and CDK6 leading to G1-S cell cycle progression. The fundamental unit of lymphatic tissues is the lymphatic nodule, which consists of a germinal center with an outer ring or mantle of small lymphocytes, which is the initial location of the cells of this lymphoma. Previous standard therapies for mantle cell lymphoma include (i) the rituximab-CHOP regimen of cyclophosphamide, hydroxydaunorubicin (doxorubicin), oncovin (vincristine), and prednisone combined with rituximab, (ii) cyclophosphamide, oncovin, hydroxydaunorubicin, dexamethasone, cytarabine, and methotrexate, (iii) bortezomib, or (iv) lenalidomide.

Pirtobrutinib is a pyrazole carboxamide derivative (Fig. 4B) that is FDA-approved for the third-line treatment of mantle cell lymphoma, chronic lymphocytic leukemia, and small lymphocytic lymphoma (Table 2). Gomez et al. solved the X-ray crystal structure of pirtobrutinib bound to BTK [78]. They reported that the drug formed two hydrogen bonds with the third hinge residue (M477), one hydrogen bond with the first hinge residue (E475), and one hydrogen bond with the preceding residue (T474) (Fig. 5B). The compound makes hydrophobic contact with three shell residues (Sh1/2/3), three regulatory spine residues (RS2/3/4), and three catalytic spine residues (CS6/7/8). Pirtobrutinib also makes hydrophobic contact with L408 of the β1-strand, G409 of the GRL, AxK-K430, F442 of the αC-helix, Q459 of the back loop, M477 and C481 of the hinge-linker segment, DFG-D539, and G541 and L542 of the activation segment. Modi and Dunbrack found that this enzyme occurs

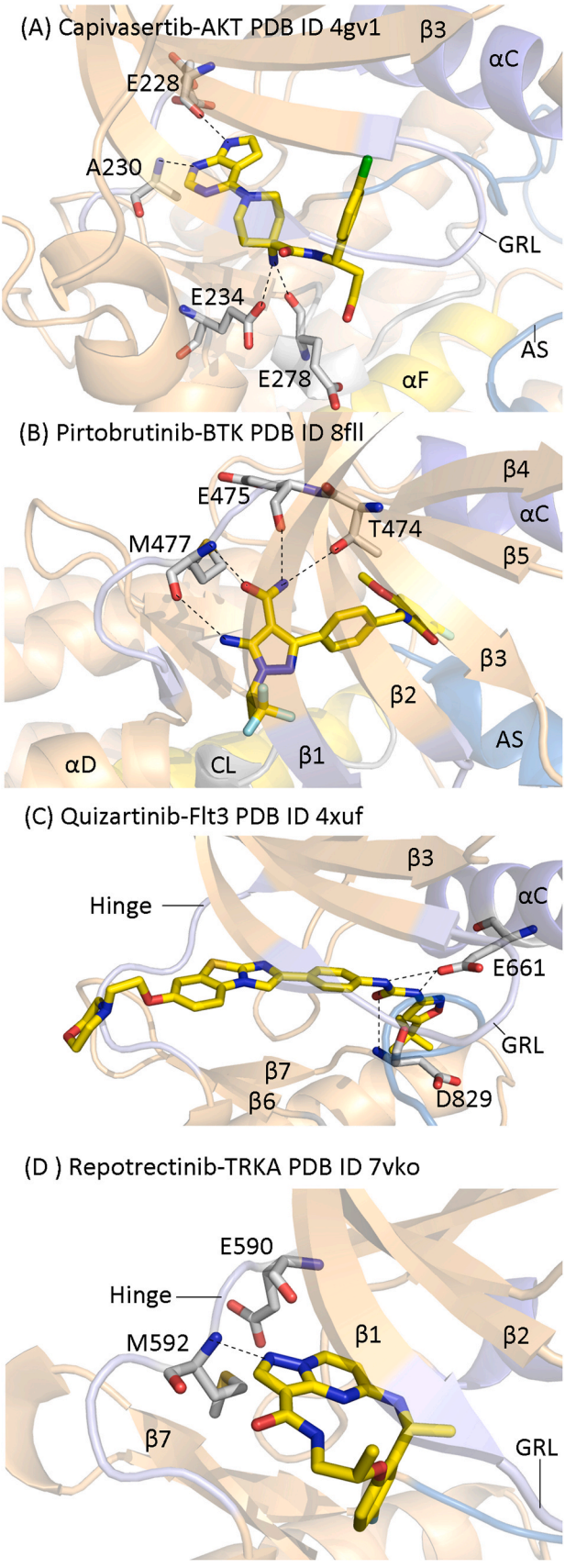

Fig. 5. (A) Capivasertib-AKT. (B) Pirtobrutinib-BTK. (C) Quizartinib-Flt3. (D) Repotrectinib-TRKA. The respective PDB ID numbers are listed. The drug carbon atoms are colored yellow and the dashed lines represent polar bonds. CL, catalytic loop; GRL, glycine-rich loop.

within the inactive BLBplus enzyme cluster with the DFG-D_{in} conformation, which they label as a type 1.5_Front Allosteric inhibitor [29]. The drug is found in the front pocket, gate area, back pocket and BP-I-A/B and BP-II-in subpockets and we classify this compound as a type I½ A inhibitor because it is an inactive DFG-D_{in} structure that extends into the back pocket [33]. See Ref. [7] for a summary of its properties and the clinical trials that led to its FDA-approval.

4.3. *Quizartinib and Flt3*

Studies on Flt3 began after the discovery of a feline sarcoma virus in 1971 by McDonough et al. [79]. The viral oncogene is called v-FMS (feline McDonough sarcoma) virus and subsequent work led to the discovery of the c-FMS proto-oncogene or colony-stimulating factor-1 receptor (CSF1R) [46]. Flt1 (fms-like tyrosine kinase-1) is VEGFR1 and Flt2 is fibroblast growth factor receptor-1 (FGFR1). Flt3 (fms-like tyrosine kinase-3) is a receptor protein-tyrosine kinase that plays a crucial role in normal hematopoiesis. This receptor, which is expressed by early lymphoid and myeloid progenitor cells, regulates the proliferation and differentiation of hematopoietic cells. Flt3 is not expressed in mature hematopoietic cells. *FLT3* mutations are found in about one-third of newly diagnosed acute myelogenous leukemia (AML) patients. *FLT3* internal tandem duplication (ITD) mutations result from the head-to-tail duplication of one up to 412 amino acids within the juxtamembrane domain and such mutations occur in about 20–25% of patients with AML. The most common sites for duplication occur within the tyrosine-rich region involving codons 589 to 599. Moreover, *FLT3* tyrosine kinase (*FLT3 TK*) mutations, usually within the activation segment, occur in 5–10% of AML patients.

Flt3, PDGFRα/β, Kit, and the macrophage/colony stimulating factor-1 receptor are type III receptor protein-tyrosine kinases. See Ref. [80] for a description of the properties of the 20 types of receptor protein-tyrosine kinases. The type III receptors contain an extracellular segment, a transmembrane segment, an intracellular domain that consists of a juxtamembrane segment, a protein kinase domain that contains an insert of several amino acid residues, and a C-terminal tail. The extracellular portion contains five immunoglobulin-like domains (D1–D5). The important residues in human Flt3 are listed in Table 3. The extracellular segment, which contains 517 amino acid residues, is longer than the intracellular domain, which contains 430 residues. Additionally, the C-terminal tail contains 50 amino acids (944−993). The human Flt3L (Flt3 ligand) consists of 235 residues, the amino-terminal 26 residues of which make up the signal peptide. Membrane associated Flt3L contains 209 residues. It can undergo proteolysis as catalyzed by ADAM17 (A Disintegrin And Metalloproteinase) [8] to generate a soluble form consisting of 178 residues that form active dimers. Membrane-associated and soluble Flt3L are equipotent growth factors.

The Flt3 ligand, which promotes dimerization and activation of Flt3, is a noncovalent dimer that results from hydrophobic and polar interactions [46]. The dimeric ligand interacts with the D3 portion of two Flt3 receptors with a K_d value of 0.2–0.5 nM. This interaction promotes the phosphorylation of residues in the autoinhibitory JM domain and relieves this inhibition. Additional phosphorylation reactions occur elsewhere that lead to the binding of proteins that promote the activation of the MAP kinase and PKB/AKT signaling modules that result in cell proliferation. See Ref. [46] for a comprehensive discussion of Flt3-mediated signal transduction. Y842 in the activation segment of Flt3 undergoes phosphorylation. Unlike many protein-tyrosine kinases, phosphorylation of a tyrosine residue within the activation segment is not required for the attainment of maximal Flt3 enzyme activity.

Acute myelogenous leukemia (AML) is a malignancy of hematopoietic progenitor cells with a variable clinical course. The expected number of new cases in the United States in 2023 is 20,380 and the number of deaths is projected to be 13,310 [16]. This represents about 1.04% of all cancer cases and 1.85% of all cancer deaths. The incidence of AML is about twice that of chronic myelogenous leukemia (CML) with

8930 new cases and a projected number of deaths in 2023 of 1310 (note the lower death rate for CML as a result of the introduction of imatinib and other BCR-Abl antagonists in the treatment of this disorder). Most of the signs and symptoms in patients with AML result from the replacement of normal bone marrow cells with malignant cells. The patients' chief complaint may be fatigue, which is often accompanied by easy bruising, bleeding, and fever [7]. Laboratory findings include an abnormal bone marrow cytology with at least 20% blasts, usually accompanied with an elevated peripheral white blood cell count with blasts as well as thrombocytopenia (decreased platelet count) and anemia.

Treatment is divided into two phases: (i) remission-induction therapy (to attain remission) and (ii) post-remission or consolidation therapy (to maintain remission) [9]. Remission-induction therapy involves a combination of an anthracycline (daunorubicin or idarubicin) and cytarabine. The anthracyclines intercalate with DNA, inhibit the progression of topoisomerase II, and inhibit replication. Cytarabine is converted into cytosine arabinoside triphosphate and it is incorporated into DNA where it results in the inhibition of both DNA and RNA biosynthesis. The anthracyclines are administered intravenously over a seven-day period while cytarabine is given by a bolus intravenous injection during each of the first three days of this period (the conventional 7 + 3 regimen). This therapy produces complete remission in 80–90% of patients less than 60 years of age and in 50–60% of older patients. Complete remission refers to the normalization of the bone marrow and peripheral blood count, but it is not synonymous with a cure. Complete remission may be followed by allogeneic stem cell transplantation. Quizartinib is FDA-approved to be given in combination with the above remission-induction and consolidation therapies.

Quizartinib is a benzothiazole phenylurea derivative (Fig. 4C) that is FDA-approved for the combination treatment with standard cytarabine and anthracycline induction and cytarabine consolidation and as maintenance monotherapy following consolidation chemotherapy for the treatment of adult patients with newly diagnosed acute myeloid leukemia (AML) that is *FLT3* internal tandem duplication-positive as detected by an FDA-approved test as described in the FDA label. Zorn et al. determined the X-ray crystal structure of quizartinib bound to Flt3 [81]. They observed that the urea N–H groups hydrogen bonded with the αC-E661 and the urea oxygen hydrogen-bonded with the backbone N–H group of DFG-D829 (Fig. 5C). The medicinal makes hydrophobic contact with RS1 (L292), RS2 (F293), RS3 (L202), Sh1 (T211), the gatekeeper (M227), and CS6 (M281), CS7 (V164), and CS8 (A177). Quizartinib also makes hydrophobic contact with L616 of the β1-strand, AxK-K644, E661 and M664 of the αC-helix, I674 of the back loop, ^{693}YCCYG^{697} of the hinge-linker, I827 of the β8-strand, C828 (the x of xDFG), DFG-D829, and A833 of the activation segment. Modi and Dunbrack found that this enzyme occurs within the inactive BBAminus enzyme cluster with the DFG-D_{out} conformation, which they label as a type II inhibitor [29]. The drug is found in the front pocket, gate area, back pocket, and BP-I-B, BP-II-out, and BP-III and we classify this compound as a type IIA inhibitor because it has the DFG-D_{out} conformation and extends into the back pocket [33]. The interaction of this drug with its target is very unusual because it fails to hydrogen bond with any of the hinge residues. See Ref. [82] for a summary of quizartinib pre-clinical studies and clinical trials.

4.4. Properties of repotrectinib

Repotrectinib is a macrocyclic pyrazolo[1,5-*a*]pyrimidine derivative (Fig. 4D) that is FDA-approved for the treatment of ROS1-positive NSCLC (Table 2). The compound was designed to overcome on-target acquired ROS1-inhibitor resistance mutations, especially against those occurring in the enzyme solvent front. This compound is a potent inhibitor of ROS1, ALK, and NTRKA/B/C [83]. These five proteins are receptor protein-tyrosine kinases. Repotrectinib demonstrated potent enzymatic inhibition activities against wildtype ROS1 (IC_{50} = 0.0706 nM), ROS1 *G2032R* (IC_{50} =0.456 nM) and ROS1 *D2033N* (IC_{50} = 0.236 nM). The inhibitory activities are preserved in cellular inhibition assays with IC_{50} values < 0.2 nM, 3.3 nM, and 1.3 nM against wildtype CD74-ROS1, CD74-ROS1 *G2032R*, and CD74-ROS1 *D2033N* transfected Ba/F3 cells, respectively. Studies with the TRK family indicate that repotrectinib is most potent against TRKC with an IC_{50} of 0.211 nM, followed by TRKB (IC_{50} = 0.297 nM) and TRKA (IC_{50} = 0.533 nM), respectively. The NTRK proteins are NeuroTrophic Receptor Kinases that respond to nerve growth factor.

Unfortunately, we lack the X-ray crystal structure of repotrectinib bound to ROS1, but we have the structure of this agent bound to NTRKA (Fig. 5D), which we describe here. Murray et al. reported that repotrectinib forms a hydrogen bond with E590 and M592 of the hinge [84]. However, the data indicate that the donor and acceptor atoms to E590 are 3.7 Å apart, a distance too long for a hydrogen bond to form (upper limit of 3.3 Å). The drug makes hydrophobic contact with two shell residues (Sh1 and Sh2) and four catalytic spine residues (CS4/6/7/8). The agent also interacts hydrophobically with L516 at the end of the β1-strand, G517 of the GRL, AxK-K544, F589 (the gatekeeper residue), E590, Y591, M592, G595, and D596 of the hinge-linker segment, R654 and N655 of the catalytic loop, and G677 (the x of xDFG). Modi and Dunbrack do not ascribe this drug-enzyme complex to any of their clusters. The compound occupies the front pocket and FP-I of a DFG-D_{in}-αC_{out} inactive enzyme. Because the drug fails to occupy the back pocket of an inactive DFG-D_{in} complex, we classify the interaction as that of a type I½ B inhibitor [33]. See Refs. [83,85] for a summary of the development of repotrectinib and for the results of clinical trials that led to its approval in 2023.

5. Small molecule FDA-approved kinase antagonists lacking a drug-enzyme structure

5.1. Fruquintinib, a VEGFR2 blocker used for the management of metastatic colorectal cancer

Colorectal cancer (CRC) is the third most common cancer in men and the second most common in women [86]. The estimated incidence of this disorder in the United States in 2023 is 153,020 (81,860 men and 71,160 women) and the estimated number of deaths is 52,550 (28,470 men and 24,080 women). Early-stage CRC patients are asymptomatic, but about one-quarter already have metastatic disease at the time of diagnosis [87]. The five-year survival of patients with metastatic disease is less than 20%. The main treatments for early-stage CRC patients are surgery, radiotherapy, and chemotherapy. For patients with metastatic disease, first- and second-line treatments typically involve oxaliplatin or irinotecan combined with a fluoropyrimidine (5-fluorouracil or capecitabine), often in combination with a targeted drug therapy including (i) a VEGFR inhibitor or (ii) an EGFR inhibitor in patients with wild-type RAS. However, most patients with metastatic disease eventually become nonresponsive, insensitive, or intolerant to these treatments, leading to the need for third-line therapies. Therefore, the choice of appropriate treatment options plays a crucial role in prolonging survival. Regorafenib was the first small-molecule kinase inhibitor approved for the third-line treatment of metastatic CRC. It improves patient survival by inhibiting multiple growth-promoting protein kinases involved in tumor cell production, tumor angiogenesis, and maintenance of the tumor microenvironment.

Fruquintinib is a dimethoxyquinazoline (Fig. 4E) that is indicated for the third-line treatment of adult patients with metastatic colorectal cancer who have been previously treated with fluoropyrimidine-, oxaliplatin-, and irinotecan-based chemotherapy, an anti-VEGF therapy, and an anti-EGFR therapy – as described in the FDA label. Its IC_{50} values for VEGFR1/2/3 are 33/35/0.5 nM, respectively [88]. Fruquintinib, a selective oral protein-tyrosine kinase inhibitor, gained global approval for the first time in China in 2018 for the treatment of patients with metastatic disease who have failed at least a second-line therapy [89].

The drug led to increases in both overall survival (OS) and progression-free survival (PFS). See Ref. [90] for additional information on the clinical trials that led to the approval of fruquintinib in the United States.

5.2. Momelotinib, a JAK1/2 and ACVR1 inhibitor approved for the treatment of myelofibrosis

Myelofibrosis (MF) is a rare myeloproliferative neoplasm characterized by bone marrow fibrosis, anemia, splenomegaly, and constitutional symptoms such as fever and night sweats. The malady is uncommon with an annual incidence of about 3000 cases per year in the United States [91]. Constitutional symptoms triggered by cytokine overproduction cause a significant burden in the health-related quality of life in patients diagnosed with this chronic and progressive illness. Symptom burden has also been associated with poor prognosis and overall survival. The manifestation of myelofibrosis symptoms is heterogeneous because some patients may experience none, some, or all common symptoms in differing degrees of severity.

Myelofibrosis arises de novo (primary myelofibrosis) or secondarily to polycythemia vera or essential thrombocythemia [92]. Myelofibrosis presents with constitutional symptoms and fatigue, which are accompanied by splenomegaly and either cytopenias (an abnormally low cell count) or cytoses (an abnormally high cell count). The most frequent cytopenia is anemia (a deficiency of erythrocytes), which correlates with a poorer prognosis. Anemic patients often require red blood cell transfusions. People with myelofibrosis often exhibit severe cachexia with loss of muscle mass along with bone pain, splenic infarcts, pruritus, thrombosis, and bleeding. Patients with myelofibrosis are rarely eligible for curative hematopoietic stem-cell transplantation, an intervention with high morbidity and mortality. The FDA-approved JAK1/2 inhibitors, ruxolitinib and fedratinib, reduce spleen size and constitutional symptoms, but produce the on-target toxicities of anemia and thrombocytopenia.

Momelotinib is a pyrimidine-benzamide (Fig. 4F) multikinase inhibitor indicated for the treatment of intermediate or high-risk myelofibrosis, including primary or secondary disease (post-polycythemia vera or post-essential thrombocythemia), in adults with anemia (Table 2). The multikinase inhibitor blocks the JAK nonreceptor protein-tyrosine kinases and ACVR1, a bone morphogenetic protein (BMP) receptor protein-serine/threonine kinase [93,94]. The IC_{50} of momelotinib for JAK1/2/3 and TYK2 was 11/18/155 nM and 17 nM, respectively [93]. Its IC_{50} value for ACVR1 was 8 nM [94]. The BMP receptor controls the production of hepcidin (an iron metabolism regulator) through activation of the hepatic BMP–SMAD pathway [93]. ACVR1 is a transmembrane protein-serine/threonine kinase belonging to the transforming growth factor-β superfamily. Signaling through ACVR1 is intricate and involves various ligands including activins and BMPs. Receptor activation leads to SMAD signaling, nuclear translocation, and regulation of transcription where SMAD is the acronym for Suppressor of Mothers Against Decapentaplegic, a transcription factor family. Momelotinib blockade of ACVR1 down regulates hepcidin expression and results in the increased mobilization of cellular iron stores resulting in the improvement of the anemia. See Ref. [93] for information on the clinical trials that led to the approval of momelotinib.

5.3. Ritlecitinib, a JAK3 antagonist used for the management of alopecia areata

Alopecia areata, which is an autoimmune hair loss disorder affecting children and adults, is characterized by the destruction of hair follicles by dysregulated immune cells [95]. This disorder is difficult to treat and is characterized by recurring stages of hair regrowth and hair loss. It can be exacerbated by anxiety and stress with an adverse impact on the patient quality of life. Alopecia areata is characterized by patches of hair loss on the scalp, while in patients with more severe disease there may be a complete loss of hair on the scalp (alopecia totalis) or entire body (alopecia universalis). Topical or intralesional corticosteroids and topical sensitizers were the primary treatments available for mild disease, while oral corticosteroids (methyl-prednisone), methotrexate, and azathioprine were prescribed for patients with severe disease [96]. These treatments are characterized by low efficacy and better modalities of treatment are needed.

Ritlecitinib is a pyrrolo[2,3-*d*]pyrimidine derivative (Fig. 4G) that is a JAK3 inhibitor that is FDA-approved for the treatment of severe alopecia areata in adults and adolescents 12 years and older (www.brimr.org/PKI/PKIs.htm). It is not recommended for use in combination with other JAK inhibitors, biologic immunomodulators, cyclosporine, or other potent immunosuppressants. It carries several black box warnings against various infections (bacterial, fungal, viral, opportunistic), sudden cardiovascular death, malignancies including lymphomas and lung cancer, and pulmonary embolism and other thromboembolic phenomena. Ritlecitinib irreversibly and specifically inhibits Janus kinase 3 (JAK3) and members of the TEC protein-tyrosine kinase family, which include TEC, BTK, ITK, BMX, and TXK [95]. The kinases of the JAK family activate signal transducers and activators of transcription (STATs). The JAK/STAT pathway is involved in the upregulation of interferon-γ and interleukin-15 (IL-15), which stimulate and activate the $CD8^+$ T cells. The $CD8^+$ T cells attack hair follicle cells and this is implicated in the pathogenesis of alopecia areata. In addition, the TEC kinase family also contributes to the cytolytic function of natural killer cells and $CD8^+$ T cells. The ritlecitinib blockade of the TEC family kinases, primarily expressed in hematopoietic cells, further impedes the immune attack on the hair follicles and brings about an anti-inflammatory response. Thus, ritlecitinib, with its dual inhibition, reduces hair loss and stimulates hair regrowth. The extent of hair loss in ritlecitinib clinical trials was measured by a routine dermatological procedure using the SALT (Severity of Alopecia Tool) score. The drug demonstrated good clinical efficacy and a favorable safety profile despite the black box warnings [95]. See Refs. [95–97] for a summary of the clinical trials that led to the FDA-approval of ritlecitinib.

6. Physicochemical properties of orally effective drugs

6.1. Lipinski's rule of five (Ro5)

Pharmacologists and medicinal chemists have studied the physicochemical properties of drugs that are orally bioavailable to learn how to develop additional orally effective agents. Lipinski's rule of five (Ro5) is an experimental and computational procedure that is used to characterize membrane permeability, solubility, and efficacy in the drug-discovery setting [98]. It is a rule of thumb that evaluates drug-likeness and determines whether an agent with specific pharmacological activities has characteristics suggesting that it would be orally bioavailable. The Lipinski criteria were based on data showing that most orally efficacious medicines are relatively small and moderately lipophilic agents. The Ro5 criteria are used during drug discovery and development as pharmacologically active lead compounds are systematically optimized to improve their activity while maintaining selectivity.

The Ro5 criteria indicate that less than ideal oral effectiveness is more likely to occur when (i) the atom-based calculated Log P (ALogP) is greater than 5, when (ii) there are more than 5 hydrogen-bond donors, when (iii) there are more than 5 × 2 or 10 hydrogen-bond acceptors, and when (iv) the molecular weight is more than 5 × 100 or 500 [98]. The partition coefficient (P) is the ratio of the solubility of the un-ionized drug in the organic phase divided by its solubility in the aqueous phase of water-saturated *n*-octanol. The P value reflects the hydrophobicity of a compound; the greater the P value, the greater the hydrophobicity. The number of hydrogen-bond donors is the sum of NH and OH groups. The number of hydrogen-bond acceptors is somewhat more difficult to assess; these are the number of neutral heteroatoms except for halogen

atoms, heteroaromatic oxygen and sulfur atoms, pyrrole nitrogen atoms, and higher oxidation states of nitrogen, phosphorus, and sulfur, but they include the oxygen atoms bonded to them. The Ro5 criteria were based on the physicochemical properties of more than two thousand reference medicines [98].

Excluding the macrolides (everolimus, sirolimus, and temsirolimus), the average molecular weight (MW) of the orally effective FDA-approved protein kinase inhibitors is 472 ranging from 285 (ritlecitinib) to 615 (trametinib) (Table 7). The compounds with a molecular weight greater than 500 include the three macrolides and 25 other drugs. Although this data suggests that there is a tendency for orally bioavailable small molecule protein kinase antagonists to exceed the 500 Da molecular-weight criterion, the masses of the larger compounds excepting the macrolides are near 500 Da. Moreover, 18 of the 80 approved drugs have an ALogP of greater than five; these exceptions do not include capivasertib, fruquintinib, momelotinib, pirtobrutinib, quizartinib, repotrectinib, ritlecitinib – the newly approved medicinals described in this review. Moreover, tepotinib and trilaciclib have more than five hydrogen bond donors and dabrafenib and fostamatinib have more than ten hydrogen bond acceptors. Overall, a total of 37 of the 80 FDA-approved small molecule protein kinase inhibitors fail to conform to Lipinski's Ro5. Of these 37, bosutinib, brigatinib, cabozantinib, entrectinib, fostamatinib, infigratinib, lapatinib, midostaurin, mobocertinib, neratinib, nilotinib, ripretinib have two Ro5 deficiencies with a molecular weight greater than 500 and a partition coefficient greater than 5. Dabrafenib has three Ro5 deficiencies with a molecular weight greater than 500, an ALogP greater than five, and 11 hydrogen bond acceptors. These are FDA-approved agents, but finding drug candidates during the discovery process with two or three Ro5 criteria exceptions is normally an unwanted finding.

6.2. The importance of lipophilicity and ligand efficiency

6.2.1. Lipophilic efficiency, LipE

After the publication of Lipinski's Ro5 in 2001 [98], subsequent examination of the chemical and physical properties of orally effective agents has led to various refinements [99–106]. For example, lipophilic efficiency, or LipE, is an attribute that is used in drug discovery that combines potency and lipophilic-mediated binding as a tactic to increase binding efficacy. The following expressions are used to compute lipophilic efficiency:

$$\text{LipE} = \text{p}IC_{50} - \text{ALogP};\ \text{LipE} = \text{p}K_i - \text{ALogP}$$

Like its usage to designate the molar hydrogen ion concentration as pH, the operator p denotes the negative of the Log of the IC_{50} or K_i. Moreover, ALogP is an atom-based computed Log of the partition coefficient; this parameter expresses the ratio of drug solubility in the organic phase divided by its solubility in the aqueous phase of immiscible *n*-octanol/water.

The second term of the equation (– ALogP or minus ALogP) reflects the lipophilicity of a compound and the value is computed using an algorithm based upon the characteristics of thousands of reference organic compounds. The greater the solubility of a drug in the organic phase when compared with the aqueous phase of a *n*-octanol/water mixture, the greater is its lipophilicity. Leeson and Springthorpe reported that drug lipophilicity, as assessed by its – ALogP value, is a key property that should be monitored during drug development [100]. Their use of – ALogP was based upon observations made before the calculation of the distribution coefficient (D) became more common. The distribution coefficient ($LogD_{7.4}$) is the ratio of the solubility of the ionized and un-ionized compound in the organic phase over the aqueous phase of immiscible *n*-octanol/water at a specified pH of the aqueous phase, which is usually 7.4. In general, either ALogP or $LogD_{7.4}$ can be used to monitor several compounds in the same investigation. Note that large negative – ALogP values in the defining formula decrease the lipophilic efficiency.

A high lipophilicity may promote the binding of a drug to adventitious targets and this binding may increase toxicity. One objective during drug discovery is to increase potency without concurrently increasing lipophilicity. The use of lipophilic efficiency assists in the optimization of lead compounds by directly comparing a series of drug congeners; moreover, the same procedure for determining the lipophilic efficiency should be used to ensure that such comparisons are valid [102,103]. To cite a cogent example, Cui et al. described the optimization of lead compounds during the development of crizotinib using lipophilic efficiency as an index of binding effectiveness [107]; crizotinib is FDA-approved for the management of ALK-positive and ROS1-positive NSCLC.

The ALogP of various compounds can be calculated in seconds to minutes. Because experimental measurements of LogP are labor intensive, such measurements are carried out only in select cases. Hopkins et al. reported that reasonable values for LogP are less than ~ 3 and those of lipophilic efficiency are greater than ~ 5 [102]. Increasing the potency and decreasing the lipophilicity during drug development generally produces agents with better pharmacological properties in vivo. The average value of lipophilic efficiency (LipE) for 77 FDA-approved small molecule protein kinase blockers (omitting the three macrolides) is 4.53 with a range from 1.3 (neratinib) to 7.96 (deucravacitinib) (Table 8). The average value for ALogP for the 77 FDA-approved drugs (excluding the three macrolides) was 3.97 with a range from 1.1 (baricitinib) to 6.36 (ceritinib).

6.2.2. Ligand efficiency, LE

The ligand efficiency (LE) relates potency, or binding affinity, to the number of heavy (nonhydrogen) atoms of a drug. The following formula is used to compute this property:

$$\text{LE} = \Delta G^{\circ\prime}/\text{N} = -\text{RT}\ \ln K_{eq}/\text{N} = -2{\cdot}303\text{RT}\ \text{Log}\ K_{eq}/\text{N}$$

$\Delta G^{\circ\prime}$ is the standard free energy change of a ligand binding to its target enzyme at neutral pH, R denotes the universal gas constant or energy-temperature coefficient (1.98×10^{-3} kcal/degree-mol), T represents the temperature in degrees Kelvin, K_{eq} is the value of the equilibrium constant, and N represents the number of heavy (nonhydrogen) atoms in the drug. The K_i or IC_{50} values represent surrogates for the equilibrium constant. At a physiological temperature of 37 °C (310 K), this equation becomes $-(2.303 \times (1.98 \times 10^{-3}/\text{K}) \times 310\ \text{K}\ \text{Log}\ K_{eq})/\text{N}$ or – 1.41 Log K_{eq}/N. Other investigators use a temperature of 300 K and the multiplication factor becomes – 1.37 [102,106]. Ligand efficiency reflects ligand affinities based upon the average binding energy per atom. Furthermore, ligand efficiency is quite helpful in fragment-based drug discovery protocols and, like lipophilic efficiency, it facilitates the selection of congeners of lead compounds for further development [103].

Ligand efficiency reflects the binding affinity per heavy atom of the ligand or drug of interest. The value of N is a surrogate for the molecular weight. The equation used to calculate ligand efficiency shows that its value is directly proportional to – Log K_{eq} (a positive number), or the binding affinity, and is inversely proportional to the number of nonhydrogen atoms. Hopkins et al. indicated that optimal values for ligand efficiency (LE) should be greater than 0.3 kcal per mol per nonhydrogen atom [99,102]. Ligand efficiency values for the FDA-approved small molecule protein kinase blockers based upon representative K_i or IC_{50} values are included in Table 8. The average value for ligand efficiency for 77 of the FDA-approved protein kinase inhibitors (excluding the three macrolides) was 0.361 with a range from 0.237 (mobocertinib) to 0.558 (tofacitinib). Five drugs had values of less than 0.3 including mobocertinib, midostaurin, neratinib, nilotinib, and pacritinib. The values for ligand efficiency (LE) and lipophilic efficiency (LipE) listed in Table 8 are based on data acquired under different experimental conditions. Accordingly, these values cannot be used to make a direct

Table 7
Properties of FDA-approved small molecule inhibitors.

Drug	PubMED CID	MW (Da)	HD[a]	HA[b]	ALogP[c]	Log $D_{7.4}$[d]	PSA (Å^2)[e]	nStereo[f]	Cplx[g]
Abemaciclib	46220502	507	1	9	4.94	3.76	75	0	723
Abrocitinib	78323835	323	2	6	1.3	0.79	99.4	0	474
Acalabrutinib	71226662	466	2	6	3.31	2.56	119	1	845
Afatinib	10184653	486	2	8	4.39	2.34	88.6	1	702
Alectinib	49806720	483	1	5	4.77	4.75	72.4	0	867
Asciminib	72165228	450	3	8	3.46	3.86	103	1	626
Avapritinib	118023034	499	1	9	2.61	2.12	106	1	752
Axitinib	6450551	386	2	4	4.64	4.15	96	0	557
Baricitinib	44205240	371	1	7	1.10	-0.19	129	0	678
Belumosudil	11950170	452	3	6	4.82	4.02	105	0	678
Binimetinib	10288191	441	3	7	3.01	3.81	88.4	0	521
Bosutinib	5328940	530	1	8	5.19	3.37	82.9	0	734
Brigatinib	68165256	584	2	9	5.09	2.49	85.9	0	835
Cabozantinib	25102847	501	2	7	5.54	4.65	98.8	0	795
Capivasertib	25227436	429	4	6	2.10	–0.16	120	0	580
Capmatinib	25145656	412	1	6	3.43	2.96	81.5	0	637
Ceritinib	57379345	558	3	8	6.36	3.38	114	0	835
Cobimetinib	16222096	531	3	7	3.78	2.73	64.6	1	624
Crizotinib	11626560	450	2	6	5.04	0.95	78	1	558
Dabrafenib	44462760	520	2	11	5.36	5.10	148	0	817
Dacomitinib	11511120	470	2	7	5.16	3.53	79.4	0	665
Dasatinib	3062316	488	3	9	3.31	3.74	135	0	642
Deucravacitinib	134821691	426	3	8	1.78	2.10	136	0	648
Encorafenib	50922675	540	3	10	3.91	2.61	149	1	836
Entrectinib	25141092	561	3	8	5.03	4.87	85.5	0	847
Erdafitinib	67462786	446	1	7	4.18	1.25	77.3	0	583
Erlotinib	176870	393	1	7	3.41	3.20	74.7	0	525
Everolimus	6442177	958	3	14	6.20	7.40	205	15	1810
Fedratinib	16722836	525	3	9	4.82	3.23	117	0	787
Fostamatinib	11671467	580	4	15	3.09	-0.52	187	0	904
Fruquintinib	44480399	393	1	7	3.85	2.64	95.7	0	579
Futibatinib	71621331	418	1	7	1.78	1.54	108	1	723
Gefitinib	123631	447	1	8	4.28	3.64	68.7	0	545
Gilteritinib	49803313	552	3	10	2.70	1.69	121	0	785
Ibrutinib	24821094	441	1	6	4.22	3.63	99.2	1	678
Imatinib	5291	494	2	7	4.59	3.80	86.3	0	706
Infigratinib	53235510	560	2	8	5.35	3.99	95.1	0	724
Lapatinib	208908	580	2	9	6.14	4.40	115	0	898
Larotrectinib	46188928	428	2	7	2.95	2.44	86	2	659
Lenvatinib	9823820	427	3	5	4.07	2.52	116	0	634
Lorlatinib	71731823	406	1	7	2.80	1.62	110	1	700
Midostaurin	9829523	571	1	4	5.91	5.43	77.7	4	1140
Mobocertinib	118607832	586	2	9	5.08	3.79	114	0	935
Momelotinib	25062766	414	2	7	2.98	2.70	103	0	615
Neratinib	9915743	557	2	8	5.93	3.05	112	0	881
Netarsudil	66599893	454	2	5	4.89	3.42	94.3	1	678
Nilotinib	644241	530	2	9	6.36	5.35	97.6	0	817
Nintedanib	135423438	540	2	7	3.62	2.57	102	0	892
Osimertinib	71496458	500	2	7	4.51	3.01	87.6	0	752
Pacritinib	46216796	473	1	7	4.96	3.11	68.7	0	644
Palbociclib	5330286	448	2	8	2.97	1.30	103	0	775
Pazopanib	10113978	438	2	8	3.14	3.55	127	0	717
Pemigatinib	86705695	487	1	8	3.66	1.80	83.2	0	731
Pexidartinib	25151352	417	2	7	5.23	3.35	66.5	0	537
Pirtobrutinib	129269915	479	3	9	3.43	4.55	125	1	719
Ponatinib	24826799	533	1	8	4.46	4.54	65.8	0	910
Pralsetinib	129073603	534	3	9	4.20	3.64	136	1	816
Quizartinib	24889392	561	2	9	5.86	5.05	106	0	849
Regorafenib	11167602	483	3	8	5.69	4.49	92.4	0	686
Repotrectinib	135565923	355	2	6	2.55	2.17	80.6	0	524
Ribociclib	44631912	435	2	7	2.80	0.91	91.2	0	636
Ripretinib	71584930	510	3	5	5.67	4.38	86.4	0	746
Ritlecitinib	118115473	285	2	4	1.94	1.40	73.9	2	402
Ruxolitinib	25126798	306	1	4	3.47	2.48	83.2	1	453
Selpercatinib	134436906	526	1	9	3.28	3.11	112	0	885
Selumetinib	10127622	458	3	6	3.53	4.27	88.4	0	523
Sirolimus	5284616	914	3	13	6.18	7.45	195	15	1760
Sorafenib	216239	465	3	7	5.55	4.34	92.4	0	646
Sunitinib	5329102	398	3	4	3.33	1.28	77.2	0	636
Temsirolimus	6918289	1030	4	16	4.39	?	242	15	2010
Tepotinib	25171648	493	0	7	4.01	2.26	94.7	0	880
Tivozanib	9911830	455	2	7	5.64	4.16	108	0	631
Tofacitinib	9926791	312	1	5	1.54	1.19	88.9	2	488
Trametinib	11707110	615	2	6	3.94	3.18	102	0	1090

(*continued on next page*)

Table 7 (*continued*)

Drug	PubMED CID	MW (Da)	HD[a]	HA[b]	ALogP[c]	Log $D_{7.4}$[d]	PSA (Å^2)[e]	nStereo[f]	Cplx[g]
Trilaciclib	68029832	447	2	7	2.72	2.29	91.2	0	707
Tucatinib	51039094	481	2	8	5.09	5.25	111	0	796
Upadacitinib	58557659	380	2	6	2.91	0.85	78.3	2	561
Vandetanib	3081361	475	1	7	5.00	2.81	59.5	0	539
Vemurafenib	42611257	490	2	7	5.54	4.61	100	0	790
Zanubrutinib	135565884	472	2	5	4.22	3.42	103	0	756

[a] HD, no. of hydrogen bond donors.
[b] HA, no. of hydrogen bond acceptors.
[c] ALogP, values for atom-based log of the partition coefficient from https://www.ebi.ac.uk/chembl/.
[d] Log $D_{7.4}$, values for the log of the distribution coefficients at pH 7.4 obtained from https://www.ebi.ac.uk/chembl/.
[e] PSA, polar surface area obtained from https://pubchem.ncbi.nlm.nih.gov/.
[f] Defined atom stereocenter count.
[g] Complexity values obtained from https://pubchem.ncbi.nlm.nih.gov/.

comparison of the drugs because different procedures were used to obtain the data. These findings were acquired from various drug development projects and provide only representative values.

6.2.3. *Additional chemical descriptors of orally effective drugs*

To decipher drug properties related to oral bioavailability, not-unexpectedly, the Ro5 has generated many variations and corollaries. For example, Veber et al. found that the polar surface area (PSA) and the number of rotatable bonds differs between orally active and inactive compounds for a large series of drugs in rats [104]. They reported that the optimal number of rotatable bonds is 10 or less. This parameter regulates passive membrane permeation and reflects molecular flexibility (degrees of freedom). Furthermore, the molecular flexibility is related to the entropy change that results from ligand binding and determines in part the amount of drug bound to its targets. With the exceptions of four drugs with 11 rotatable bonds (erlotinib, fedratinib, lapatinib, neratinib) and mobocertinib with 13 rotatable bonds, the remaining 80 drugs (the macrolides were excluded) have 10 or fewer of these bonds (Table 8). The average value is 6.34 and the number of rotatable bonds ranges from 0 (lorlatinib, repotrectinib) to 13 (mobocertinib). Furthermore, Veber et al. reported that medicinals with a polar surface area less than or equal to 140 Å^2 are orally effective [104]. This parameter represents the sum of the surface over all polar atoms, primarily oxygen and nitrogen, and it also includes any connected hydrogen atoms. Excluding the three macrolides, the average value for the surface area is 98.5 Å^2 with a range from 59.5 (vandetanib) to 187 (fostamatinib). Fostamatinib, encorafenib, and dabrafenib are the only drugs with a polar surface area exceeding 140 Å^2 (Table 7). Furthermore, Oprea reported that the number of ring structures (both aromatic and nonaromatic) in most orally approved drugs is three or greater [101]. All approved small molecule protein kinase blockers have three or more rings with an average value of 4.25 and a range from three (14 drugs) to seven (midostaurin) (Table 8). Except for temsirolimus and trilaciclib (which are given intravenously) and netarsudil (an eye drop), all of the FDA-approved drugs listed are orally effective. Furthermore, ruxolitinib is used both orally and topically.

The molecular complexity of a compound is based upon the elements it contains, its structural features, and its symmetry. The complexity is calculated with the Bertz/Hendrickson/Ihlenfelt algorithm [108,109]. It is based upon the nature and number of the constituent atoms, the bonding pattern, and the type of the chemical bonds (single, double, triple, aromatic). Molecular complexity ranges from 0 for simple ions to several thousand for elaborate natural products. Larger compounds generally have a greater molecular complexity value than smaller compounds. Contrariwise, chemicals containing few elements and those that are highly symmetrical have a smaller molecular complexity value. The molecular complexity values for the drugs in this article were acquired from PubChem (https://pubchem.ncbi.nlm.nih.gov/). For the 80 FDA-approved kinase inhibitors, the mean complexity value is 753 with a range from 402 (ritlecitinib) to 2010 (temsirolimus) (Table 7). As expected, the three large macrolide compounds possess the greatest molecular complexity values. There are no recommended or optimal molecular complexity values for orally bioavailable drugs; however, this parameter may be helpful in predicting the ease or difficulty of drug synthesis, an important consideration in the production of commercial pharmaceutical agents. Similarly, the occurrence of stereocenters in drugs may make drug synthesis more difficult.

Leeson et al. compared drug properties in two time frames: 1990–2009 and 2010–2020 [106]. They found that the lipophilicity and molecular weight of approved drugs increased with time. We compared the averages of selected properties of FDA-approved protein kinase antagonists during two-time frames: 1999 – 2012 and 2013 – 2023. This analysis excluded the three large macrolides. We observed an increase in the average molecular weight (457 to 476 Da), polar surface area (91 to 101 Å^2), heavy atom count (32.3 to 34.6), and complexity (663 to 726). However, the average number of hydrogen bond donors and acceptors, ALopP, the number of rotatable bonds, the ring count, ligand efficiency, lipophilic efficiency, and the potency (K_i value) were essentially unchanged (Tables 7 and 8). Leeson et al. reported that the molecular weight of all FDA-approved drugs, including protein kinase antagonists, has increased over time [106].

Ritchie and Macdonald examined the role of aromaticity on its effect on the pharmacological properties of various agents in the context of drug design and discovery [110]. Aromaticity refers to cyclically conjugated compounds with a stability that is substantially greater than that of a localized Kekulé structure because of electron delocalization. They considered aromatic bicyclic and tricyclic structures as containing two and three aromatic rings, respectively. The aromatic ring count includes structures containing carbon and various heteroatoms. These authors reported that increasing the number of carboaromatic rings had a detrimental effect on pharmacologic efficacy by increasing binding to serum albumin, decreasing aqueous solubility, and inhibiting cytochrome P450. We find that the average number of aromatic rings in the 80-approved protein kinase antagonists was 3.4 and the mean number of benzene moieties was 1.10 (Table 8). All of the FDA-approved kinase antagonists with the exception of the three macrolides have a minimum of two aromatic rings and a maximum of five. Sixteen of the drugs lacked benzene moieties and the number of drugs possessing one or two benzenes was about evenly distributed among the remainder (Table 8).

Bayliss et al. evaluated the dose and water solubility for orally effective drug and drug candidates [111]. They reported that daily doses of 100 mg or less reduced the risk of toxicity. The range of dosages for protein kinase blockers given orally is from 1.34 mg to 1920 mg daily with an average of about 300 mg (Table 8). The daily doses range from 1.34, 2, and 2 mg for tivozanib, trametinib, and baricitinib and 1200, 1250, and 1920 mg for alectinib, lapatinib, and vemurafenib, respectively. Only 30 of the 77 orally bioavailable FDA-approved kinase inhibitors have doses of 100 mg or less. Bayliss et al. reported that agents with a solubility in water of 100 μg/ml or less are associated with an increased risk of failure during clinical trials and drug development

Table 8
Properties of FDA-approved small molecule protein kinases inhibitors.

Drug	Target, kinase family[a]	K_i nM[b]	pK_i	LipE[c]	N * [d]	LE[e]	Dose[f]	Sol[g]	nRotB[h]	nRng[i]	nAr[j]	nBnz[k]	QED[l]
Abemaciclib	CDK4, S/T	0.6	9.22	4.28	37	0.351	400 *	15.9	7	5	4	0	0.38
Abrocitinib	JAK1, NRY	5.1	8.29	7.04	22	0.531	100	420	6	3	2	0	0.83
Acalbrutinib	BTK, NRY	3.1	8.51	5.20	35	0.343	200 *	10.9	4	5	4	1	0.45
Afatinib	EGFR, RY	0.5	9.33	4.94	34	0.387	40	12.8	8	4	3	1	0.46
Alectinib	ALK, RY	1.9	8.72	3.95	36	0.342	1200 *	10.5	3	6	3	0	0.58
Asciminib	BCR-Abl, NRY	0.5	9.3	5.84	31	0.300	80	55	6	4	3	1	0.50
Avapritinib	PDGFRα, RY	0.18	9.7	7.09	37	0.370	300	30.1	5	6	5	1	0.39
Axitinib	VEGFR2, RY	0.25	9.6	4.96	28	0.483	300	0.55	5	4	4	1	0.52
Baricitinib	JAK2, NRY	7	8.15	7.05	26	0.442	2	357	5	4	3	0	0.72
Belumosudil	ROCK2, S/T	53.9	7.3	2.48	34	0.303	200	2.89	7	5	5	1	0.33
Binimetinib	MEK1, DS	12	7.92	4.91	27	0.414	90 *	49.9	6	3	3	1	0.40
Bosutinib	BCR-Abl, NRY	20	7.7	2.51	36	0.302	500	9.5	9	4	3	1	0.38
Brigatinib	ALK, RY	0.398	9.4	4.31	40	0.331	180	22	8	5	3	2	0.35
Cabozantinib	RET, RY	5	8.3	2.76	37	0.316	40	1.99	8	5	4	2	0.31
Capivasertib	AKT=PKB, S/T	3	8.52	6.42	30	0.400	800	> 1000	6	4	3	1	0.48
Capmatinib	MET, RY	0.13	9.89	6.46	31	0.450	800 *	5.29	4	5	5	1	0.49
Ceritinib	ALK, RY	0.2	9.7	3.34	38	0.360	750	2.22	9	4	3	2	0.28
Cobimetinib	MEK1, DS	0.79	9.1	5.32	30	0.428	60	42.2	4	4	2	2	0.53
Crizotinib	ALK, RY	0.63	9.2	4.16	30	0.432	500 *	6.11	5	4	3	1	0.53
Dabrafenib	BRAF, S/T	0.4	9.4	4.04	35	0.379	300 *	3.27	6	4	4	2	0.37
Dacomitinib	EGFR, RY	2	8.7	3.54	33	0.372	45	8.74	7	4	3	1	0.47
Dasatinib	BCR-Abl, NRY	0.16	9.8	6.49	33	0.419	100	12.8	7	4	3	1	0.47
Deucravacitinib	TYK2, NRY	0.2	9.69	7.96	31	0.441	6	0.159	7	4	3	1	0.52
Encorafenib	BRAF, S/T	0.3	9.52	5.61	36	0.373	450	11.2	10	3	3	1	0.37
Entrectinib	TRKA, RY	1	9	3.97	41	0.310	600	8.9	7	6	4	2	0.29
Erdafitinib	FGFR1, RY	2	8.7	4.52	33	0.372	8	13	9	4	4	1	0.41
Erlotinib	EGFR, RY	0.32	9.5	6.09	29	0.462	150	8.91	11	3	3	1	0.42
Everolimus	FKBP12/mTOR, S/T	?	?	?	68	?	10	1.63	9	3	0	0	0.13
Fedratinib	JAK2, NRY	6	8.22	3.40	37	0.313	400	9.49	11	4	3	2	0.35
Fostamatinib	SYK, RY	17	7.77	4.68	40	0.274	300 *	52	10	4	3	1	0.26
Fruquintinib	VEGFR2, RY	35	7.46	3.61	29	0.363	5	0.0803	5	4	4	0	0.55
Futibatinib	FGFR2, RY	4	8.4	6.62	31	0.382	20	40	6	4	3	1	0.51
Gefitinib	EGFR, RY	0.5	9.3	5.02	31	0.423	250	27	8	4	3	1	0.52
Gilteritinib	Flt3, RY	0.41	9.39	6.69	40	0.331	120	22.3	9	5	2	1	0.43
Ibrutinib	BTK, NRY	12.6	7.9	3.68	33	0.338	560	20.3	5	5	4	2	0.47
Imatinib	BCR-Abl, NRY	1	9	4.41	37	0.343	600	14.6	7	5	4	2	0.39
Infigratinib	FGFRs, RY	5	8.3	2.95	38	0.308	125	29.9	8	4	3	2	0.38
Lapatinib	EGFR, RY	1	9	2.86	40	0.317	1250	22.3	11	5	5	2	0.18
Larotrectinib	TRK, RY	9.7	8.01	5.06	31	0.364	200 *	238	3	5	3	1	0.67
Lenvatinib	VEGFR2, RY	3.98	8.4	4.33	30	0.395	24	6.22	6	4	3	1	0.55
Lorlatinib	ALK, RY	9	8.05	5.25	30	0.378	100	108	0	3	3	1	0.61
Midostaurin	Flt3, RY	37	7.43	1.52	43	0.244	200 *	15.7	3	7	4	1	0.29
Mobocertinib	EGFR, RY	60	7.22	2.14	43	0.237	160	13.6	13	4	4	1	0.17
Momelotinib	JAK2/1, NRY	1.4	8.85	5.87	31	0.402	200	32.5	6	4	3	2	0.06
Neratinib	ErbB2/HER2, RY	59	7.23	1.30	40	0.255	240	6.74	11	4	4	1	0.22
Netarsudil	ROCK1/2, S/T	1	9	4.11	34	0.373	0.01	0.23	8	4	4	2	0.39
Nilotinib	BCR-Abl, NRY	12.5	7.9	1.54	39	0.286	600 *	2.01	6	5	5	2	0.27
Nintedanib	FGFR, RY	39.8	7.4	3.78	40	0.261	300 *	30.9	8	5	4	2	0.35
Osimertinib	EGFR, RY	7	8.15	3.64	37	0.311	80	22.4	10	4	4	1	0.31
Pacritinib	JAK2, NRY	19	7.72	2.21	35	0.289	100	38	4	4	2	1	0.54
Palbociclib	CDK4, S/T	10	8	5.03	33	0.342	125	17.4	5	5	3	0	0.58
Pazopanib	VEGFR2, RY	30	7.52	4.38	31	0.342	800	43.3	5	4	4	1	0.49
Pemigatinib	FGFR, RY	0.5	9.3	5.64	35	0.375	13.5	144	6	5	3	1	0.57
Pexidartinib	CSF1R, RY	13	7.89	2.66	29	0.384	800 *	3.15	5	4	4	0	0.47
Pirtobrutinib	BTK, NRY	0.5	9.3	5.87	34	0.386	200	3.84	7	3	3	2	0.45
Ponatinib	BCR-Abl, NRY	1	9	4.54	39	0.325	45	2.95	8	5	4	2	0.39
Pralsetinib	RET, RY	0.5	9.3	5.10	39	0.336	400	10.1	8	5	4	0	0.31
Quizartinib	Flt3, RY	3.3	8.48	2.62	40	0.299	35.4	50.9	8	5	3	1	0.26
Regorafenib	VEGFR2, RY	4.2	8.4	2.71	33	0.359	160	1.02	5	3	3	2	0.41
Repotrectinib	ROS1, RY	0.07	11.2	8.60	26	0.607	320 *	49.8	3	3	3	1	0.65
Ribociclib	CDK4, S/T	10	8	5.20	32	0.353	600	231	5	5	3	0	0.64
Ripretinib	RET, RY	3	8.52	2.85	33	0.364	150	5.83	5	4	4	2	0.32
Ritlecitinib	JAK3, NRY	33.1	7.48	5.54	21	0.502	50	457	3	3	2	0	0.85
Ruxolitinib	JAK1, NRY	1.2	8.92	5.45	23	0.547	20 *	116	4	4	3	0	0.8
Selpercatinib	RET, RY	1	9	5.72	39	0.325	320 *	29.9	8	4	4	0	0.37
Selumetinib	MEK1, DS	14	7.85	4.32	27	0.410	80 *	21	6	3	3	1	0.39
Sirolimus	FKBP12/mTOR, S/T	?	?	?	65	?	2	1.73	6	3	0	0	0.16
Sorafenib	VEGFR1, RY	15.8	7.8	2.25	32	0.344	800 *	1.71	5	3	3	2	0.46
Sunitinib	VEGFR2, RY	3.98	8.4	5.07	29	0.408	50	30.8	7	3	2	0	0.63
Temsirolimus	FKBP12/mTOR, S/T	?	?	?	73	?	25 * *	2.35	11	4	0	0	?
Tepotinib	MET, RY	1	9	4.99	37	0.343	450	?	7	5	4	2	0.38
Tivozanib	VEGFR2, RY	6.5	8.19	2.55	37	0.312	1.34	52.1	6	4	4	1	0.39
Tofacitinib	JAK1, NRY	0.79	9.1	7.56	23	0.558	10 *	299	3	3	2	0	0.93
Trametinib	MEK1, DS	3.4	8.47	4.53	37	0.323	2	30.7	5	5	3	2	0.33

(*continued on next page*)

Table 8 (*continued*)

Drug	Target, kinase family[a]	K_i nM[b]	pK_i	LipE[c]	N * [d]	LE[e]	Dose[f]	Sol[g]	nRotB[h]	nRng[i]	nAr[j]	nBnz[k]	QED[l]
Trilaciclib	CDK4/6, S/T	1	9	6.28	33	0.385	480	260	3	6	3	0	0.64
Tucatinib	ErbB2/HER2, RY	8	8.1	3.01	36	0.317	600 *	4	6	6	5	1	0.36
Upadacitinib	JAK1, NRY	43	7.37	4.46	27	0.385	15	70.7	3	4	3	0	0.73
Vandetanib	RET, RY	50	7.3	2.30	30	0.343	300	10.2	6	4	3	1	0.54
Vemurafenib	BRAF, S/T	3.98	8.4	2.86	33	0.359	1920 *	0.36	7	4	4	2	0.33
Zanubrutinib	BTK, NRY	0.3	9.52	5.30	35	0.384	320 *	10.3	6	5	3	2	0.52

[a] NRY, non-receptor protein-tyrosine kinase; RY, receptor protein-tyrosine kinase; S/T, protein-serine/threonine kinase; DS; dual specificity protein kinase (catalyzes protein-tyrosine and then threonine phosphorylation of target kinase activation segments but evolutionarily in the protein-serine/threonine kinase family).
[b] Representative values obtained from www.ebi.ac.ug/chembl/ and from klifs.net.
[c] LipE (lipophilic efficiency) = $p\mathrm{IC}_{50}$ – ALogP
[d] N * , Number of heavy (nonhydrogen) atoms.
[e] LE (ligand efficiency) = – 2.303 RT Log_{10} K_i/N where N is the number of heavy (non-hydrogen) atoms in the drug
[f] Dosage in mg/day from FDA label; * , one-half of total daily dose taken twice per day; * *, once weekly.
[g] Sol, solubility (μg/ml) in water (go.drugbank.com/drugs/)
[h] nRotB, number of Rotatable bonds.
[i] nRng, number of rings
[j] nAr, number of Aromatic rings
[k] nBnz, number of benzene moieties
[l] QED, summed, weighted desirability (scores using MW + ALogP + HBD + HBA + PSA + nRotB + nAr) obtained from https://www.ebi.ac.uk/chembl/; see Ref. [106] for a full explanation.

[111]. We tallied the solubility of the FDA-approved protein kinase blockers in water and found a range from 0.36 μg/ml (vemurafenib) to 420 μg/ml for the abrocitinib with a mean value of about 50 μg/ml. This calculation excludes capivasertib and tepotinib; the former is freely soluble in water and there is no information in the public domain on the solubility of tepotinib. Only 11 of the 80 drugs including capivasertib have a solubility greater than 100 μg/ml. The range in solubilities and dosages among the FDA-approved drugs is nearly three orders of magnitude.

7. Epilogue and perspective

Although substantial progress has been made in the discovery and development of orally bioavailable small molecule protein kinase inhibitors since the FDA-approval of imatinib in 2001, this field is still in its infancy. Oprea et al. suggested that the altered expression of many understudied protein kinases may play an important role in tumorigenesis [112]. Moreover, these understudied proteins may be valuable drug targets. Examples include eukaryotic elongation factor 2 kinase (EEF2K), cyclin-dependent protein kinase 12 (CDK12), and mitogen-activated protein kinase kinase kinase 1 (MAP3K1). Most (69) of the FDA-approved kinase antagonists are antineoplastic while most of the other blockers function as immunomodulators [10,113–116]. Owing to the inherent genetic changes in neoplastic cells, resistance to protein kinase inhibitors develops on a nearly universal basis. This resistance prompted the development of second, third, and later generation antagonists that target the initial enzyme and malignancy. Moreover, acquired drug resistance is often the result of gatekeeper mutations in the initial protein kinase target [3]. A gatekeeper mutation in *EGFR* (*T790M*) is a case in point and this is the third most commonly observed protein kinase mutation. Furthermore, it accounts for about half of all acquired *EGFR* inhibitor resistance mutations.

Because 244 protein kinase genes map to disease loci or cancer amplicons [8], it is likely that (i) a significant increase in the number of drugs blocking more protein kinases will be developed and (ii) new medicinals will be formulated for the management of additional illnesses [117–120]. Adding new protein kinase targets to the therapeutic armamentarium will require the elucidation of signaling modules besides the RAS-RAF-MEK MAP kinase and phosphatidylinositol 3-kinase/AKT/mTOR signaling pathways [121]. Along with the 80 approved protein kinase antagonists reviewed in this article, the FDA has approved five drugs that inhibit phosphatidylinositol 3-kinases (PI3Ks are members of the atypical protein kinase family) [9]. These include alpelisib – an orally bioavailable PI3K-α inhibitor that is used for the treatment of breast cancer – and copanlisib, duvelisib, idelalisib, and umbralisib that are orally bioavailable PI3K-δ inhibitors that are prescribed for the third-line treatment of follicular lymphomas and other hematological diseases. As the protein kinase antagonist discipline develops, it is likely that protein kinase blockers with new pharmacophores, chemotypes, and scaffolds will be fabricated [122]. Asciminib is a unique type IV allosteric inhibitor that binds directly to its drug target. The macrolides (everolimus, sirolimus, and temsirolimus) are type IV allosteric inhibitors that bind to FKBP12 and the drug-protein complex inhibits the catalytic activity of the mTOR protein-serine/threonine kinase; these three drugs are indirect blockers of their target protein kinase and not direct inhibitors like asciminib [123]. We anticipate that additional allosteric inhibitors will be developed that antagonize novel enzymes that are part of several protein kinase signal transduction pathways [124]. Furthermore, it is likely that new irreversible inhibitors that target protein kinases with –SH groups near the ATP-binding site will be forthcoming.

Of the 80 FDA-approved drugs, receptor protein-tyrosine kinases are the chief targets of 44 of them followed by nonreceptor protein-tyrosine kinases (20), protein-serine/threonine kinases (12), and dual-specificity protein kinases (4) (Table 1). Members of the EGFR/ErbB family represent the top-ranked targets followed by the JAK, VEGFR, BCR-Abl, ALK, and FGFR families. CDK4/6 is targeted by four of the FDA-approved antagonists that are prescribed for the treatment of breast cancer. The dual specificity (MEK1/2) protein kinases, which block the RAS-RAF-MEK MAP kinase pathway, include binimetinib (used in combination with encorafenib for the management of melanoma), cobimetinib (used in combination with vemurafenib for the treatment of melanoma), trametinib (used in combination with dabrafenib for the treatment of melanoma, NSCLC with *BRAF V600E/K* mutations, and advanced thyroid cancer), and selumetinib (prescribed for the management of neurofibromatosis I or Von Recklinghausen disease).

The clinical efficacy of drugs that are FDA-approved for the treatment of chronic myelogenous leukemia (CML) is vastly superior to other protein kinase antagonists that are used for the treatment of other disorders. Patients with CML treated with BCR-Abl blockers have an annual mortality rate of 0.5% or less when compared with age-matched normal groups [125,126]. This means that BCR-Abl antagonists normalize the life span of CML patients. Imatinib (first generation), bosutinib, dasatinib, and nilotinib (second generation) are approved by the FDA for frontline therapy while ponatinib (third generation) is approved for resistant disease with a *T315I* mutation or after failure with at least two other protein-tyrosine kinase antagonists [127]. Asciminib is a STAMP (Specifically Targeting the Abl Myristoyl Pocket) inhibitor approved as a

third-line treatment for CML and as a first-line treatment of patients with the *T315I* mutation [116]. Several clinical trials using the combination of asciminib with bosutinib, imatinib, or nilotinib are currently underway (ClinicalTrials.gov).

The aims of the treatment of CML are to promote patient survival and to attain treatment-free remission (TFR) whenever possible [47]. For promoting survival, frontline treatment with imatinib, bosutinib, dasatinib, or nilotinib are all effective. If imatinib therapy is used for frontline treatment, a change in therapy at the first indication of resistant disease is now the standard practice. One reason for using imatinib initially is its availability as a generic agent with a cost that is lower than that of the other drugs. The choice of the second line treatment is guided by an assessment of possible mutations of the Abl kinase domain and by the patient's age and co-morbidities [126]. Side effects produced by bosutinib include diarrhea (10–30%, which is mild and self-limited) and liver and kidney dysfunction. Dasatinib can lead to occasional pulmonary hypertension (1–2%), pleural effusions (10–15%), and myelosuppression (10–20%). Nilotinib can produce hyperglycemia (10–15%), exacerbate diabetes mellitus (5–10%), and produce pancreatitis (1–3%). Ponatinib leads to the most serious side effects including vasospastic disease (10–15%), hypertension (20–30%), skin rashes (5–10%), and pancreatitis (5%) [126].

Attaining treatment-free (TFR) remission is appropriate in younger patients in order to avoid lifelong drug therapy. A deep molecular response (DMR), which is defined as a 4–4.5 log reduction in the BCR-Abl-1 transcripts on the International Scale (the ratio of BCR-Abl1 transcripts to Abl1 transcripts), is one criterion for discontinuing drug treatment. Discontinuing drug therapy after a deep molecular response lasting (i) two-to-three years is associated with a treatment-free remission rate of 50–60% and (ii) five years is associated with a treatment-free remission rate of 80%. When it is not achieved, patients fortunately respond to the therapy used before drug withdrawal. For further information on methods for producing treatment-free remission, see Refs. [126,128,129]. The concept of treatment-free remission for CML was unthinkable at the beginning of the targeted protein kinase therapy era. In the first decade of the 21st century, the idea that drug treatment for CML could be discontinued and the disease would remain abated was a pipedream.

CRediT authorship contribution statement

Roskoski Robert: Conceptualization, Data curation, Investigation, Methodology, Writing – original draft, Writing – review & editing.

Declaration of Competing Interest

The author is unaware of any affiliations, memberships, or financial holdings that might be perceived as affecting the objectivity of this review.

Acknowledgments

I thank Dr. Albert J. Kooistra for providing the template depicted in Fig. 3 and Laura M. Roskoski for providing editorial and bibliographic assistance. I also thank Jasper Martinsek and Josie Rudnicki for their help in preparing the figures and W.S. Sheppard and Pasha Brezina for their help in structural analyses. The colored figures in this paper were evaluated to ensure that their perception was accurately conveyed to colorblind readers [130].

Appendix A. Supporting information

Supplementary data associated with this article can be found in the online version at doi:10.1016/j.phrs.2024.107059.

References

[1] P. Cohen, Protein kinases – the major drug targets of the twenty-first century? Nat. Rev. Drug Discov. 1 (2002) 309–315, https://doi.org/10.1038/nrd773.
[2] R. Roskoski Jr., A historical overview of protein kinases and their targeted small molecule inhibitors, Pharm. Res 100 (2015) 1–23, https://doi.org/10.1016/j.phrs.2015.07.010.
[3] P. Cohen, D. Cross, P.A. Jänne, Kinase drug discovery 20 years after imatinib: progress and future directions, Nat. Rev. Drug Discov. 20 (2021) 551–569, https://doi.org/10.1038/s41573-021-00195-4.
[4] M.M. Attwood, D. Fabbro, A.V. Sokolov, S. Knapp, H.B. Schiöth, Trends in kinase drug discovery: targets, indications and inhibitor design, Nat. Rev. Drug Discov. 20 (2021) 839–861, https://doi.org/10.1038/s41573-021-00252-y. Author correction. Nat Rev Drug Discov 2021;20:798. doi: 10.1038/s41573-021-00303-4.
[5] G.K. Kanev, C. de Graaf, I.J.P. de Esch, R. Leurs, T. Würdinger, B.A. Westerman, A.J. Kooistra, The landscape of atypical and eukaryotic protein kinases, Trends Pharm. Sci. 40 (2019) 818–832, https://doi.org/10.1016/j.tips.2019.09.002.
[6] F. Carles, S. Bourg, C. Meyer, P. Bonnet, PKIDB: a curated, annotated and updated database of protein kinase inhibitors in clinical trials, pii: E908, Molecules 23 (2018), https://doi.org/10.3390/molecules23040908.
[7] G.M. Nitulescu, G. Stancov, O.C. Seremet, G. Nitulescu, D.P. Mihai, C.G. Duta-Bratu, S.F. Barbuceanu, O.T. Olaru, The importance of the pyrazole scaffold in the design of protein kinases inhibitors as targeted anticancer therapies, Molecules 28 (2023) 5359, https://doi.org/10.3390/molecules28145359.
[8] G. Manning, D.B. Whyte, R. Martinez, T. Hunter, S. Sudarsanam, The protein kinase complement of the human genome, Science 298 (2002) 1912–1934, https://doi.org/10.1126/science.1075762.
[9] R. Roskoski Jr., Properties of FDA-approved small molecule phosphatidylinositol 3-kinase inhibitors prescribed for the treatment of malignancies, Pharm. Res 168 (2021) 105579, https://doi.org/10.1016/j.phrs.2021.105579.
[10] R. Roskoski Jr., Properties of FDA-approved small molecule protein kinase inhibitors, Pharm. Res. 144 (2019) 19–50, https://doi.org/10.1016/j.phrs.2019.03.006.
[11] R. Roskoski Jr., Properties of FDA-approved small molecule protein kinase inhibitors: a 2020 update, Pharm. Res 152 (2020) 104609, https://doi.org/10.1016/j.phrs.2019.104609.
[12] R. Roskoski Jr., Properties of FDA-approved small molecule protein kinase inhibitors: a 2021 update, Pharm. Res 165 (2021) 105463, https://doi.org/10.1016/j.phrs.2021.105463.
[13] R. Roskoski Jr., Properties of FDA-approved small molecule protein kinase inhibitors: a 2022 update, Pharm. Res 175 (2022) 106037, https://doi.org/10.1016/j.phrs.2021.106037.
[14] S.H. Myers, V.G. Brunton, A. Unciti-Broceta, AXL inhibitors in cancer: a medicinal chemistry perspective, J. Med. Chem. 59 (2016) 3593–3608, https://doi.org/10.1021/acs.jmedchem.5b01273.
[15] B.L. Roth, D.J. Sheffler, W.K. Kroeze, Magic shotguns versus magic bullets: selectively non-selective drugs for mood disorders and schizophrenia, Nat. Rev. Drug Discov. 3 (2004) 353–359, https://doi.org/10.1038/nrd1346.
[16] R. Roskoski Jr., Orally effective FDA-approved protein kinase targeted covalent inhibitors (TCIs), Pharm. Res 165 (2021) 105422, https://doi.org/10.1016/j.phrs.2021.105422.
[17] R. Roskoski Jr., Properties of FDA-approved small molecule protein kinase inhibitors: a 2023 update, Pharm. Res. 2023 Pharm. Res 187 (2023) 106552, https://doi.org/10.1016/j.phrs.2022.106552.
[18] D.R. Knighton, J.H. Zheng, L.F. Ten Eyck, V.A. Ashford, N.H. Xuong, S.S. Taylor, J.M. Sowadski, Crystal structure of the catalytic subunit of cyclic adenosine monophosphate-dependent protein kinase, Science 253 (1991) 407–414, https://doi.org/10.1126/science.1862342.
[19] A.P. Kornev, S.S. Taylor, Dynamics-driven allostery in protein kinases, Trends Biochem Sci. 40 (2015) 628–647, https://doi.org/10.1016/j.tibs.2015.09.002.
[20] S.S. Taylor, J. Wu, J.G.H. Bruystens, J.C. Del Rio, T.W. Lu, A.P. Kornev, L.F. Ten Eyck, From structure to the dynamic regulation of a molecular switch: a journey over 3 decades, J. Biol. Chem. 296 (2021) 100746, https://doi.org/10.1016/j.jbc.2021.100746.
[21] R. Roskoski Jr., Cyclin-dependent protein serine/threonine kinase inhibitors as anticancer drugs, Pharm. Res 139 (2019) 471–488, https://doi.org/10.1016/j.phrs.2018.11.035.
[22] R. Roskoski Jr., Hydrophobic and polar interactions of FDA-approved small molecule protein kinase inhibitors with their target enzymes, Pharm. Res 169 (2021) 105660, https://doi.org/10.1016/j.phrs.2021.105660.
[23] S.K. Hanks, T. Hunter, Protein kinases 6. The eukaryotic protein kinase superfamily: kinase (catalytic) domain structure and classification, FASEB J. 9 (1995) 576–596.
[24] Madhusudan, E.A. Trafny, N.H. Xuong, J.A. Adams, L.F. Ten Eyck, S.S. Taylor, J. M. Sowadski, cAMP-dependent protein kinase: crystallographic insights into substrate recognition and phosphotransfer, Protein Sci. 3 (1994) 176–187, https://doi.org/10.1002/pro.5560030203.
[25] J. Zhou, J.A. Adams, Participation of ADP dissociation in the rate-determining step in cAMP-dependent protein kinase, Biochemistry 36 (1997) 15733–15738, https://doi.org/10.1021/bi971438n.
[26] P.A. Schwartz, B.W. Murray, Protein kinase biochemistry and drug discovery, Bioorg. Chem. 39 (2011) 192–210, https://doi.org/10.1016/j.bioorg.2011.07.004.

[27] A.P. Kornev, S.S. Taylor, Defining the conserved internal architecture of a protein kinase, Biochim Biophys. Acta 1804 (2010) 440–444, https://doi.org/10.1016/j.bbapap.2009.10.017.
[28] V. Modi, R.L. Dunbrack Jr., Defining a new nomenclature for the structures of active and inactive kinases, Proc. Natl. Acad. Sci. USA 116 (2019) 6818–6827, https://doi.org/10.1073/pnas.1814279116.
[29] V. Modi, R.L. Dunbrack Jr., Kincore: a web resource for structural classification of protein kinases and their inhibitors, Nucleic Acids Res 50 (2022) D654–D664, https://doi.org/10.1093/nar/gkab920.
[30] A.P. Kornev, N.M. Haste, S.S. Taylor, L.F. Eyck, Surface comparison of active and inactive protein kinases identifies a conserved activation mechanism, Proc. Natl. Acad. Sci. USA 103 (2006) 17783–17788, https://doi.org/10.1073/pnas.0607656103.
[31] A.P. Kornev, S.S. Taylor, L.F. Ten Eyck, A helix scaffold for the assembly of active protein kinases, Proc. Natl. Acad. Sci. USA 105 (2008) 14377–14382, https://doi.org/10.1073/pnas.0807988105.
[32] H.S. Meharena, P. Chang, M.M. Keshwani, K. Oruganty, A.K. Nene, N. Kannan, S. S. Taylor, A.P. Kornev, Deciphering the structural basis of eukaryotic protein kinase regulation, PLoS Biol. 11 (2013) e1001690, https://doi.org/10.1371/journal.pbio.1001680.
[33] R. Roskoski Jr., Classification of small molecule protein kinase inhibitors based upon the structures of their drug-enzyme complexes, Pharm. Res 103 (2016) 26–48, https://doi.org/10.1016/j.phrs.2015.10.021.
[34] R. Roskoski Jr., Anaplastic lymphoma kinase (ALK): structure, oncogenic activation, and pharmacological inhibition, Pharm. Res 68 (2013) 68–94, https://doi.org/10.1016/j.phrs.2012.11.007.
[35] R. Roskoski Jr., Anaplastic lymphoma kinase (ALK) inhibitors in the treatment of ALK-driven lung cancers, Pharm. Res 117 (2017) 343–356, https://doi.org/10.1016/j.phrs.2017.01.007.
[36] R. Roskoski Jr., The preclinical profile of crizotinib in the treatment of non-small cell lung cancer and other neoplastic disorders, Expert Opin. Drug Dis. 8 (2013) 1165–1179, https://doi.org/10.1517/17460441.2013.813015.
[37] R. Roskoski Jr., The ErbB/HER family of protein-tyrosine kinases and cancer, Pharm. Res. 79 (2014) 34–74, https://doi.org/10.1016/j.phrs.2013.11.002.
[38] R. Roskoski Jr., ErbB/HER protein-tyrosine kinases: Structure and small molecule inhibitors, Pharm. Res. 87 (2014) 42–59, https://doi.org/10.1016/j.phrs.2014.06.001.
[39] R. Roskoski Jr., Small molecule inhibitors targeting the EGFR/ErbB family of protein-tyrosine kinases in human cancers, Pharm. Res 139 (2019) 395–411, https://doi.org/10.1016/j.phrs.2018.11.014.
[40] R. Roskoski Jr., The role of small molecule platelet-derived growth factor receptor (PDGFR) inhibitors in the treatment of neoplastic disorders, Pharm. Res 129 (2018) 65–83, https://doi.org/10.1016/j.phrs.2018.01.021.
[41] R. Roskoski Jr., The role of fibroblast growth factor receptor (FGFR) protein-tyrosine kinase inhibitors in the treatment of cancers including those of the urinary bladder, Pharm. Res 151 (2020) 104567, https://doi.org/10.1016/j.phrs.2019.104567.
[42] R. Roskoski Jr., The role of small molecule Kit protein-tyrosine kinase inhibitors in the treatment of neoplastic disorders, Pharm. Res 133 (2018) 35–52, https://doi.org/10.1016/j.phrs.2018.04.020.
[43] R. Roskoski Jr, A. Sadeghi-Nejad, Role of RET protein-tyrosine kinase inhibitors in the treatment RET-driven thyroid and lung cancers, Pharm. Res 128 (2018) 1–17, https://doi.org/10.1016/j.phrs.2017.12.021.
[44] R. Roskoski Jr., Vascular endothelial growth factor (VEGF) and VEGF receptor inhibitors in the treatment of renal cell carcinomas, Pharm. Res 120 (2017) 116–132, https://doi.org/10.1016/j.phrs.2017.03.010.
[45] R. Roskoski Jr., ROS1 protein-tyrosine kinase inhibitors in the treatment of ROS1 fusion protein-driven non-small cell lung cancers, Pharm. Res 121 (2017) 202–212, https://doi.org/10.1016/j.phrs.2017.04.022.
[46] R. Roskoski Jr., The role of small molecule Flt3 receptor protein-tyrosine kinase inhibitors in the treatment of Flt3-positive acute myelogenous leukemias, Pharm. Res 155 (2020) 104725, https://doi.org/10.1016/j.phrs.2020.104725.
[47] R. Roskoski Jr., Targeting BCR-Abl in the treatment of Philadelphia-chromosome positive chronic myelogenous leukemia, Pharm. Res 178 (2022) 106156, https://doi.org/10.1016/j.phrs.2022.106156.
[48] R. Roskoski Jr., Janus kinase (JAK) inhibitors in the treatment of inflammatory and neoplastic diseases, Pharm. Res 111 (2016) 784–803, https://doi.org/10.1016/j.phrs.2016.07.038.
[49] R. Roskoski Jr., Janus kinase (JAK) inhibitors in the treatment of neoplastic and inflammatory disorders, Pharm. Res 183 (2022) 106362, https://doi.org/10.1016/j.phrs.2022.106362.
[50] R. Roskoski Jr., Ibrutinib inhibition of Bruton protein-tyrosine kinase (BTK) in the treatment of B cell neoplasms, Pharm. Res 113 (2016) 395–408, https://doi.org/10.1016/j.phrs.2016.09.011.
[51] R. Roskoski Jr., Src protein-tyrosine kinase structure, mechanism, and small molecule inhibitors, Pharm. Res 94 (2015) 9–25, https://doi.org/10.1016/j.phrs.2015.01.003.
[52] M.C. Frame, R. Roskoski Jr., Src family tyrosine kinases. Reference module in life sciences, Elsevier,, Amsterdam, 2017, pp. 1–11, https://doi.org/10.1016/B978-0-12-809633-8.07199-5.
[53] R. Roskoski Jr., MEK1/2 dual-specificity protein kinases: structure and regulation, Biochem Biophys. Res Commun. 417 (2012) 5–10, https://doi.org/10.1016/j.bbrc.2011.11.145.
[54] R. Roskoski Jr., Allosteric MEK1/2 inhibitors including cobimetanib and trametinib in the treatment of cutaneous melanomas, Pharm. Res 117 (2017) 20–31, https://doi.org/10.1016/j.phrs.2016.12.009.
[55] R. Roskoski Jr., Cyclin-dependent protein kinase inhibitors including palbociclib as anticancer drugs, Pharm. Res 107 (2016) 249–275, https://doi.org/10.1016/j.phrs.2016.03.012.
[56] R. Roskoski Jr., ERK1/2 MAP kinases: structure, function, and regulation, Pharm. Res 66 (2012) 105–143, https://doi.org/10.1016/j.phrs.2012.04.005.
[57] R. Roskoski Jr., Targeting ERK1/2 protein-serine/threonine kinases in human cancers, Pharm. Res 142 (2019) 151–168, https://doi.org/10.1016/j.phrs.2019.01.039.
[58] R. Roskoski Jr., Targeting oncogenic Raf protein-serine/threonine kinases in human cancers, Pharm. Res 135 (2018) 239–258, https://doi.org/10.1016/j.phrs.2018.08.013.
[59] R. Roskoski Jr., RAF protein-serine/threonine kinases: structure and regulation, Biochem Biophys. Res Commun. 399 (2010) 313–317, https://doi.org/10.1016/j.bbrc.2010.07.092.
[60] Y. Liu, K. Shah, F. Yang, L. Witucki, K.M. Shokat, A molecular gate which controls unnatural ATP analogue recognition by the tyrosine kinase v-Src, Bioorg. Med Chem. 6 (1998) 1219–1226, https://doi.org/10.1016/s0968-0896(98)00099-6.
[61] A.C. Dar, K.M. Shokat, The evolution of protein kinase inhibitors from antagonists to agonists of cellular signaling, Annu Rev. Biochem 80 (2011) 769–795, https://doi.org/10.1146/annurev-biochem-090308-173656.
[62] P.M. Ung, R. Rahman, A. Schlessinger, Redefining the protein kinase conformational space with machine learning, e2, Cell Chem. Biol. 25 (2018) 916–924, https://doi.org/10.1016/j.chembiol.2018.05.002.
[63] R. Hu, H. Xu, P. Jia, Z. Zhao, KinaseMD: kinase mutations and drug response database, Nucleic Acids Res. 49 (D1) (2021) D552–D561, https://doi.org/10.1093/nar/gkaa945.
[64] F. Zuccotto, E. Ardini, E. Casale, M. Angiolini, Through the "gatekeeper door": exploiting the active kinase conformation, J. Med. Chem. 53 (2010) 2691–2694, https://doi.org/10.1021/jm901443h.
[65] L.K. Gavrin, E. Saiah, Approaches to discover non-ATP site inhibitors, Med Chem. Commun. 4 (2013) 41–51.
[66] V. Lamba, I. Ghosh, New directions in targeting protein kinases: focusing upon true allosteric and bivalent inhibitors, Curr. Pharm. Des. 18 (2012) 2936–2945, https://doi.org/10.2174/138161212800672813.
[67] J.J. Liao, Molecular recognition of protein kinase binding pockets for design of potent and selective kinase inhibitors, J. Med Chem. 50 (2007) 409–424, https://doi.org/10.1021/jm0608107.
[68] O.P. van Linden, A.J. Kooistra, R. Leurs, I.J. de Esch, C. de Graaf, KLIFS: a knowledge-based structural database to navigate kinase-ligand interaction space, J. Med Chem. 57 (2014) 249–277, https://doi.org/10.1021/jm400378w.
[69] A.J. Kooistra, G.K. Kanev, O.P. van Linden, R. Leurs, I.J. de Esch, C. de Graaf, KLIFS: a structural kinase-ligand interaction database, Nucleic Acids Res 44 (D1) (2016) D365–D371, https://doi.org/10.1093/nar/gkv1082.
[70] G.K. Kanev, C. de Graaf, B.A. Westerman, I.J.P. de Esch, A.J. Kooistra, KLIFS: an overhaul after the first 5 years of supporting kinase research, Nucleic Acids Res. (2020) gkaa895, https://doi.org/10.1093/nar/gkaa895.
[71] B. Wienen-Schmidt, D. Schmidt, H.D. Gerber, A. Heine, H. Gohlke, G. Klebe, Surprising non-additivity of methyl groups in drug-kinase interaction, ACS Chem. Biol. 14 (2019) 2585–2594, https://doi.org/10.1021/acschembio.9b00476.
[72] D. Bajusz, G.G. Ferenczy, G.M. Keserű, Structure-based virtual screening approaches in kinase-directed drug discovery, Curr. Top. Med Chem. 17 (2017) 2235–2259, https://doi.org/10.2174/1568026617666170224121313.
[73] P. Wu, T.E. Nielsen, M.H. Clausen, FDA-approved small-molecule kinase inhibitors, Trends Pharm. Sci. 36 (2015) 422–439, https://doi.org/10.1016/j.tips.2015.04.005.
[74] C.L. Alves, H.J. Ditzel, Drugging the PI3K/AKT/mTOR pathway in ER^{+} breast cancer, Int. J. Mol. Sci. 24 (5) (2023 24) 4522, https://doi.org/10.3390/ijms24054522.
[75] M. Addie, P. Ballard, D. Buttar, C. Crafter, G. Currie, B.R. Davies, J. Debreczeni, H. Dry, P. Dudley, R. Greenwood, P.D. Johnson, J.G. Kettle, C. Lane, G. Lamont, A. Leach, R.W. Luke, J. Morris, D. Ogilvie, K. Page, M. Pass, S. Pearson, L. Ruston, Discovery of 4-amino-N-[(1S)-1-(4-chlorophenyl)-3-hydroxypropyl]-1-(7H-pyrrolo[2,3-d]pyrimidin-4-yl)piperidine-4-carboxamide (AZD5363), an orally bioavailable, potent inhibitor of Akt kinases, J. Med Chem. 56 (2013) 2059–2073, https://doi.org/10.1021/jm301762v.
[76] S. Tsukada, D.C. Saffran, D.J. Rawlings, O. Parolini, R.C. Allen, L. Cohen, et al., Deficient expression of a B cell cytoplasmic tyrosine kinase in human X-linked agammaglobulinemia, Cell 72 (1993) 279–290.
[77] O.C. Bruton, A decade with agammaglobulinemia, J. Pedia 60 (1962) 672–676, https://doi.org/10.1016/s0022-3476(62)80092-4.
[78] E.B. Gomez, K. Ebata, H.S. Randeria, M.S. Rosendahl, E.P. Cedervall, T. H. Morales, L.M. Hanson, N.E. Brown, X. Gong, J. Stephens, W. Wu, I. Lippincott, K.S. Ku, R.A. Walgren, P.B. Abada, J.A. Ballard, C.K. Allerston, B.J. Brandhuber, Preclinical characterization of pirtobrutinib, a highly selective, noncovalent (reversible) BTK inhibitor, Blood 142 (2023) 62–72, https://doi.org/10.1182/blood.2022018674.
[79] S.K. McDonough, S. Larsen, R.S. Brodey, N.D. Stock, W.D. Hardy Jr., A transmissible feline fibrosarcoma of viral origin, Cancer Res 31 (1971) 953–956.
[80] M.A. Lemmon, J. Schlessinger, Cell signaling by receptor tyrosine kinases, Cell 141 (2010) 1117–1134, https://doi.org/10.1016/j.cell.2010.06.011.
[81] J.A. Zorn, Q. Wang, E. Fujimura, T. Barros, J. Kuriyan, Crystal structure of the FLT3 kinase domain bound to the inhibitor quizartinib (AC220), PLoS One 10 (2015) e0121177, https://doi.org/10.1371/journal.pone.0121177.
[82] D. Akwata, A.L. Kempen, N. Dayal, N.R. Brauer, H.O. Sintim, Identification of a selective FLT3 inhibitor with low activity against VEGFR, FGFR, PDGFR, c-KIT,

and RET Anti-Targets, ChemMedChem (2023) e202300442, https://doi.org/10.1002/cmdc.202300442.
[83] A. Drilon, S.I. Ou, B.C. Cho, D.W. Kim, J. Lee, J.J. Lin, V.W. Zhu, M.J. Ahn, D. R. Camidge, J. Nguyen, D. Zhai, W. Deng, Z. Huang, E. Rogers, J. Liu, J. Whitten, J.K. Lim, S. Stopatschinskaja, D.M. Hyman, R.C. Doebele, J.J. Cui, A.T. Shaw, Repotrectinib (TPX-0005) is a next-generation ROS1/TRK/ALK inhibitor that potently inhibits ROS1/TRK/ALK solvent-front mutations, Cancer Discov. 8 (2018) 1227–1236, https://doi.org/10.1158/2159-8290.CD-18-0484.
[84] B.W. Murray, E. Rogers, D. Zhai, W. Deng, X. Chen, P.A. Sprengeler, X. Zhang, A. Graber, S.H. Reich, S. Stopatschinskaja, B. Solomon, B. Besse, A. Drilon, molecular characteristics of repotrectinib that enable potent inhibition of TRK fusion proteins and resistant mutations, Mol. Cancer Ther. 20 (2021) 2446–2456, https://doi.org/10.1158/1535-7163.MCT-21-0632.
[85] S.I. Ou, G.G. Hagopian, S.S. Zhang, M. Nagasaka, Comprehensive review of ROS1 tyrosine kinase inhibitors (TKIs)-classified by structural designs and mutation spectrum [solvent front mutation (G2032R) and central β-sheet 6 (Cβ6) mutation (L2086F), J. Thorac. Oncol. S1556-0864 (23) (2023) 02413–02419, https://doi.org/10.1016/j.jtho.2023.12.008.
[86] R.L. Siegel, K.D. Miller, N.S. Wagle, A. Jemal, Cancer statistics, 2023, CA Cancer J. Clin. 73 (1) (2023) 17–48, https://doi.org/10.3322/caac.21763.
[87] L. Gao, L. Tang, Z. Hu, J. Peng, X. Li, B. Liu, Comparison of the efficacy and safety of third-line treatments for metastatic colorectal cancer: a systematic review and network meta-analysis, Front Oncol. 13 (2023) 1269203, https://doi.org/10.3389/fonc.2023.1269203.
[88] Q. Sun, J. Zhou, Z. Zhang, M. Guo, J. Liang, F. Zhou, J. Long, W. Zhang, F. Yin, H. Cai, H. Yang, W. Zhang, Y. Gu, L. Ni, Y. Sai, Y. Cui, M. Zhang, M. Hong, J. Sun, Z. Yang, W. Qing, W. Su, Y. Ren, Discovery of fruquintinib, a potent and highly selective small molecule inhibitor of VEGFR 1, 2, 3 tyrosine kinases for cancer therapy, Cancer Biol. Ther. 15 (2014) 1635–1645, https://doi.org/10.4161/15384047.2014.964087.
[89] J. Li, S. Qin, R.H. Xu, L. Shen, J. Xu, Y. Bai, L. Yang, Y. Deng, Z.D. Chen, H. Zhong, H. Pan, W. Guo, Y. Shu, Y. Yuan, J. Zhou, N. Xu, T. Liu, D. Ma, C. Wu, Y. Cheng, D. Chen, W. Li, S. Sun, Z. Yu, P. Cao, H. Chen, J. Wang, S. Wang, H. Wang, S. Fan, Y. Hua, W. Su, Effect of fruquintinib vs placebo on overall survival in patients with previously treated metastatic colorectal cancer: the FRESCO randomized clinical trial, JAMA 319 (2018) 2486–2496, https://doi.org/10.1001/jama.2018.7855.
[90] A. Wang-Gillam, W. Schelman, S. Ukrainskyj, C. Chien, M. Gonzalez, Z. Yang, M. Kania, H. Yeckes-Rodin, Phase 1/1b open-label, dose-escalation study of fruquintinib in patients with advanced solid tumors in the United States, Invest N. Drugs 41 (2023) 851–860, https://doi.org/10.1007/s10637-023-01395-y.
[91] R.A. Mesa, S. Hudgens, L. Floden, C.N. Harrison, J. Palmer, V. Gupta, D. P. McLornan, M.F. McMullin, J.J. Kiladjian, L. Foltz, U. Platzbecker, M.L. Fox, A. J. Mead, D.M. Ross, S.T. Oh, A. Perkins, M.F. Leahy, S. Deheshi, R. Donahue, B. J. Klencke, S. Verstovsek, Symptomatic benefit of momelotinib in patients with myelofibrosis: Results from the SIMPLIFY phase III studies, Cancer Med 12 (2023) 10612–10624, https://doi.org/10.1002/cam4.5799.
[92] K. Ikeda, K. Ueda, Gaining MOMENTUM against anaemic myelofibrosis, Lancet 401 (10373) (2023) 248–249, https://doi.org/10.1016/S0140-6736(23)00171-X.
[93] A. Tefferi, A. Pardanani, N. Gangat, Momelotinib (JAK1/JAK2/ACVR1 inhibitor): mechanism of action, clinical trial reports, and therapeutic prospects beyond myelofibrosis, Haematologica 108 (2023) 2919–2932, https://doi.org/10.3324/haematol.2022.282612.
[94] M. Asshoff, V. Petzer, M.R. Warr, D. Haschka, P. Tymoszuk, E. Demetz, M. Seifert, W. Posch, M. Nairz, P. Maciejewski, P. Fowles, C.J. Burns, G. Smith, K.U. Wagner, G. Weiss, J.A. Whitney, I. Theurl, Momelotinib inhibits ACVR1/ALK2, decreases hepcidin production, and ameliorates anemia of chronic disease in rodents, Blood 129 (2017) 1823–1830, https://doi.org/10.1182/blood-2016-09-740092.
[95] A.K. Gupta, S.P. Ravi, K. Vincent, W. Abramovits, LITFULO™ (Ritlecitinib) capsules: a Janus kinase 3 Inhibitor for the treatment of severe alopecia areata, Skinmed 21 (2023) 434–438, eCollection 2023.
[96] T. Dainichi, M. Iwata, Y. Kaku, Alopecia areata: what's new in the diagnosis and treatment with JAK inhibitors? J. Dermatol. (2023) https://doi.org/10.1111/1346-8138.17064.
[97] T. Passeron, B. King, J. Seneschal, M. Steinhoff, A. Jabbari, M. Ohyama, D. J. Tobin, S. Randhawa, A. Winkler, J.B. Telliez, D. Martin, A. Lejeune, Inhibition of T-cell activity in alopecia areata: recent developments and new directions, Front Immunol. 14 (2023) 1243556, https://doi.org/10.3389/fimmu.2023.1243556.
[98] C.A. Lipinski, F. Lombardo, B.W. Dominy, P.J. Feeney, Experimental and computational approaches to estimate solubility and permeability in drug discovery and development settings, Adv. Drug Deliv. Rev. 46 (2001) 3–26, https://doi.org/10.1016/s0169-409x(00)00129-0.
[99] A.L. Hopkins, C.R. Groom, A. Alex, Ligand efficiency: a useful metric for lead selection, Drug Discov. Today 9 (2004) 430–431, https://doi.org/10.1016/S1359-6446(04)03069-7.
[100] P.D. Leeson, B. Springthorpe, The influence of drug-like concepts on decision-making in medicinal chemistry, Nat. Rev. Drug Discov. 6 (2007) 881–890, https://doi.org/10.1038/nrd2445.
[101] S. Ekins, N.K. Litterman, C.A. Lipinski, B.A. Bunin, Thermodynamic proxies to compensate for biases in drug discovery methods, Pharm. Res 33 (2016) 194–205, https://doi.org/10.1007/s11095-015-1779-y.
[102] A.L. Hopkins, G.M. Keserü, P.D. Leeson, D.C. Rees, C.H. Reynolds, The role of ligand efficiency metrics in drug discovery, Nat. Rev. Drug Discov. 13 (2014) 105–121, https://doi.org/10.1038/nrd4163.
[103] P.D. Leeson, Molecular inflation, attrition, and the rule of five, Adv. Drug Deliv. Rev. 101 (2016) 22–33, https://doi.org/10.1016/j.addr.2016.01.018.
[104] D.F. Veber, S.R. Johnson, H.Y. Cheng, B.R. Smith, K.W. Ward, K.D. Kopple, Molecular properties that influence the oral bioavailability of drug candidates, J. Med Chem. 45 (2002) 2615–2623, https://doi.org/10.1021/jm020017n.
[105] T.I. Oprea, Property distribution of drug-related chemical databases, J. Comput. Aided Mol. Des. 14 (2000) 251–264, https://doi.org/10.1023/a:1008130001697.
[106] P.D. Leeson, A.P. Bento, A. Gaulton, A. Hersey, E.J. Manners, C.J. Radoux, A. R. Leach, Target-based evaluation of "drug-like" properties and ligand efficiencies, J. Med. Chem. 64 (2021) 7210–7230, https://doi.org/10.1021/acs.jmedchem.1c00416.
[107] J.J. Cui, M. McTigue, M. Nambu, M. Tran-Dubé, M. Pairish, H. Shen, L. Jia, H. Cheng, J. Hoffman, P. Le, M. Jalaie, G.H. Goetz, K. Ryan, N. Grodsky, Y. L. Deng, M. Parker, S. Timofeevski, B.W. Murray, S. Yamazaki, S. Aguirre, Q. Li, H. Zou, J. Christensen, Discovery of a novel class of exquisitely selective mesenchymal-epithelial transition factor (c-MET) protein kinase inhibitors and identification of the clinical candidate 2-(4-(1-(quinolin-6-ylmethyl)-1H-[1,2,3]triazolo[4,5-*b*]pyrazin-6-yl)-1H-pyrazol-1-yl)ethanol (PF-04217903) for the treatment of cancer, J. Med. Chem. 55 (2012) 8091–8109, https://doi.org/10.1021/jm300967g.
[108] S.H. Bertz, The first general index of molecular complexity, J. Am. Chem. Soc. 1103 (1981) 3559–3601.
[109] J.B. Hendrickson, P. Huang, A.G. Toczko, Molecular complexity: a simplified formula adapted to individual atoms, J. Chem. Inf. Comput. Sci. 27 (1987) 63–67.
[110] T.J. Ritchie, S.J. Macdonald, Physicochemical descriptors of aromatic character and their use in drug discovery, J. Med Chem. 57 (2014) 7206–7215, https://doi.org/10.1021/jm500515d.
[111] M.K. Bayliss, J. Butler, P.L. Feldman, D.V. Green, P.D. Leeson, M.R. Palovich, A. J. Taylor, Quality guidelines for oral drug candidates: dose, solubility and lipophilicity, Drug Discov. Today 21 (2016) 1719–1727, https://doi.org/10.1016/j.drudis.2016.07.007.
[112] T.I. Oprea, C.G. Bologa, S. Brunak, A. Campbell, G.N. Gan, A. Gaulton, S. M. Gomez, R. Guha, A. Hersey, J. Holmes, A. Jadhav, L.J. Jensen, G.L. Johnson, A. Karlson, A.R. Leach, A. Ma'ayan, A. Malovannaya, S. Mani, S.L. Mathias, M. T. McManus, T.F. Meehan, C. von Mering, D. Muthas, D.T. Nguyen, J. P. Overington, G. Papadatos, J. Qin, C. Reich, B.L. Roth, S.C. Schürer, A. Simeonov, L.A. Sklar, N. Southall, S. Tomita, I. Tudose, O. Ursu, D. Vidovic, A. Waller, D. Westergaard, J.J. Yang, G. Zahoránszky-Köhalmi, Unexplored therapeutic opportunities in the human genome, Nat. Rev. Drug Discov. 17 (2018) 377, https://doi.org/10.1038/nrd.2018.52.
[113] L. Huang, S. Jiang, Y. Shi, Tyrosine kinase inhibitors for solid tumors in the past 20 years (2001-2020), J. Hematol. Oncol. 13 (2020) 143, https://doi.org/10.1186/s13045-020-00977-0.
[114] K. Bechman, M. Yates, J.B. Galloway, The new entries in the therapeutic armamentarium: the small molecule JAK inhibitors, Pharm. Res 147 (2019) 104392, https://doi.org/10.1016/j.phrs.2019.104392. Corrigendum doi: 10.1016/j.phrs.2020.104634.
[115] Bechman K., Galloway G.B., Winthrop K.L. Small-molecule protein kinase inhibitors and the risk of fungal infections. Curr Fungal Infect Rep. 10.1007/s12281–019-00350-w.
[116] R. Roskoski Jr., Cost in the United States of FDA-approved small molecule protein kinase inhibitors used in the treatment of neoplastic and non-neoplastic diseases, Pharm. Res. 199 (2023) 107036, https://doi.org/10.1016/j.phrs.2023.107036.
[117] C.I. Wells, H. Al-Ali, D.M. Andrews, C.R.M. Asquith, A.D. Axtman, I. Dikic, D. Ebner, P. Ettmayer, C. Fischer, M. Frederiksen, R.E. Futrell, N.S. Gray, S. B. Hatch, S. Knapp, U. Lücking, M. Michaelides, C.E. Mills, S. Müller, D. Owen, A. Picado, K.S. Saikatendu, M. Schröder, A. Stolz, M. Tellechea, B.J. Turunen, S. Vilar, J. Wang, W.J. Zuercher, T.M. Willson, D.H. Drewry, The kinase chemogenomic set (KCGS): an open science resource for kinase vulnerability identification, Int J. Mol. Sci. 22 (2021) 566, https://doi.org/10.3390/ijms22020566.
[118] J. Choo, G. Heo, C. Pothoulakis, E. Im, Posttranslational modifications as therapeutic targets for intestinal disorders, Pharm. Res. (2021) 105412, https://doi.org/10.1016/j.phrs.2020.105412.
[119] C.C. Ayala-Aguilera, T. Valero, Á. Lorente-Macías, D.J. Baillache, S. Croke, A. Unciti-Broceta, Small molecule kinase inhibitor drugs (1995-2021): medical indication, pharmacology, and synthesis, J. Med. Chem. 65 (2022) 1047–1131, https://doi.org/10.1021/acs.jmedchem.1c00963.
[120] Z. Xie, X. Yang, Y. Duan, J. Han, C. Liao, Small-molecule kinase inhibitors for the treatment of nononcologic diseases, J. Med. Chem. 64 (2021) 1283–1345.
[121] R. Roskoski Jr., Blockade of mutant RAS oncogenic signaling with a special emphasis on KRAS, Pharm. Res 172 (2021) 105806, https://doi.org/10.1016/j.phrs.2021.105806.
[122] A. Cichońska, B. Ravikumar, R.J. Allaway, F. Wan, S. Park, O. Isayev, S. Li, M. Mason, A. Lamb, Z. Tanoli, M. Jeon, S. Kim, M. Popova, S. Capuzzi, J. Zeng, K. Dang, G. Koytiger, J. Kang, C.I. Wells, T.M. Willson, , IDG-DREAM Drug-Kinase Binding Prediction Challenge Consortium, T.I. Oprea, A. Schlessinger, D. H. Drewry, G. Stolovitzky, K. Wennerberg, J. Guinney, T. Aittokallio, Crowdsourced mapping of unexplored target space of kinase inhibitors, Nat. Commun. 12 (2021) 3307, https://doi.org/10.1038/s41467-021-23165-1.
[123] H.Y. Min, H.Y. Lee, Molecular targeted therapy for anticancer treatment, Exp. Mol. Med. (2022), https://doi.org/10.1038/s12276-022-00864-3.
[124] X. Lu, J.B. Smaill, K. Ding, New promise and opportunities for allosteric kinase inhibitors, Angew. Chem. Int. Ed. Engl. 59 (2020) 13764–13776, https://doi.org/10.1002/anie.201914525.

[125] K. Sasaki, S.S. Strom, S. O'Brien, E. Jabbour, F. Ravandi, M. Konopleva, G. Borthakur, N. Pemmaraju, N. Daver, P. Jain, S. Pierce, H. Kantarjian, J. E. Cortes, Relative survival in patients with chronic-phase chronic myeloid leukaemia in the tyrosine-kinase inhibitor era: analysis of patient data from six prospective clinical trials, Lancet Haematol. 2 (2015) e186–e193, https://doi.org/10.1016/S2352-3026(15)00048-4.

[126] H.M. Kantarjian, N. Jain, G. Garcia-Manero, M.A. Welch, F. Ravandi, W. G. Wierda, E.J. Jabbour, The cure of leukemia through the optimist's prism, Cancer 128 (2022) 240–259, https://doi.org/10.1002/cncr.33933.

[127] E. Jabbour, H. Kantarjian, J. Cortes, Use of second- and third-generation tyrosine kinase inhibitors in the treatment of chronic myeloid leukemia: an evolving treatment paradigm, Clin. Lymphoma Myeloma Leuk. 15 (2015) 323–334, https://doi.org/10.1016/j.clml.2015.03.006.

[128] J. Cortes, C. Pavlovsky, S. Saußele, Chronic myeloid leukemia. Lancet 398 (2021) 1914–1926, https://doi.org/10.1016/S0140-6736(21)01204-6.

[129] F.G. Haddad, K. Sasaki, G.C. Issa, G. Garcia-Manero, F. Ravandi, T. Kadia, J. Cortes, M. Konopleva, N. Pemmaraju, Y. Alvarado, M. Yilmaz, G. Borthakur, C. DiNardo, N. Jain, N. Daver, N.J. Short, E. Jabbour, H. Kantarjian, Treatment-free remission in patients with chronic myeloid leukemia following the discontinuation of tyrosine kinase inhibitors, Am. J. Hematol. 97 (2022) 856–864, https://doi.org/10.1002/ajh.26550.

[130] R. Roskoski Jr., Guidelines for preparing color figures for everyone including the colorblind, Pharm. Res. 119 (2017) 240–241, https://doi.org/10.1016/j.phrs.2017.02.005. Erratum in: Pharmacol Res 2019;139:569. doi: 10.1016/j.phrs.2018.09.019.